Ship Rescue Optimization: A New Metaheuristic Algorithm for Solving Engineering Problems

Shu-Chuan Chu[1], Ting-Ting Wang[1], Ali Riza Yildiz[2], Jeng-Shyang Pan[1,3]*

[1] *College of Computer Science and Engineering, Shandong University of Science and Technology, China*
[2] *Department of Automotive Engineering, Bursa Uludağ University, Turkey*
[3] *Department of Information Management, Chaoyang University of Technology, Taiwan*
scchu0803@gmail.com, 202082060058@sdust.edu.cn, profaliyildiz@gmail.com, jengshyangpan@gmail.com

Abstract

In recent years, more and more problems in the industry have started to be solved using metaheuristics. In this paper, inspired by the ship maneuvering motion function and the rescue process, we propose ship rescue optimization (SRO) to solve the challenging optimization problem. The ship rescue process can be divided into two types of delayed rescue (large area rescue) and immediate rescue (small rescue) according to the searched person, and we can correspond these two types of rescue behaviors to the search space exploration and exploitation processes, respectively. In this process, SRO simulates the motion process of ship rescue according to the ship maneuvering equation of motion and finally comes up with an optimal position update algorithm. We verified the performance of the proposed algorithm on different dimensions of 57 test functions consisting of CEC2013 and CEC2017 and on three real engineering problems, and compared it with eight current mainstream algorithms. The algorithm proposed in this paper is shown to be robustly applicable in solving challenging optimization problems.

Keywords: Metaheuristic algorithms, SRO, Ship maneuvering function

1 Introduction

At present, most problems in everyday life and in the course of scientific research can be abstracted as optimization problems. The many approaches to solving optimization problems that have been proposed over the past few decades can be broadly classified into exact and heuristic methods. Because of the drawbacks that algorithms tend to obtain only locally optimal solutions and so on, heuristic algorithms like Newton-like methods [1] and Hill-climbing method [2] are usually not used to solve complex engineering design problems. To address those drawbacks just mentioned that are difficult to overcome by traditional computational methods, researchers have further proposed meta-heuristic algorithms.

Genetic Algorithm (GA) [3], inspired by Darwinian evolution, is one of the classical algorithms in the metaheuristics. Individuals in a population are selected or eliminated based on their superiority or inferiority to fitness. In the 1990s, Italian scholars, M. Dorigo et al. proposed Ant Colony Algorithm (ACO) [4] based on ant behavior by simulating the path search behavior and used the algorithm to solve the TSP, assignment problem, jobshop scheduling problem. In 1995, the particle swarm algorithm (PSO) [6] algorithm was proposed by Eberhart and Kennedy. The algorithm simulated the predatory behavior of a flock of birds. Since then, the metaheuristic algorithm has entered a phase of rapid development. Moreover, like other evolutionary algorithms, the differential evolution algorithm (DE) [8-9] has strong global convergence and robustness by iteratively iterating and thus simulating the random wandering of biological evolution.

In addition, there are some other common algorithms, such as Bat Algorithm (BA) [5, 14], Cat Swarm Optimization (CSO) [15, 38, 43]. Phasmatodea Population Evolution (PPE) [46], etc., which derive the optimal motion formula by simulating the habits of bats, cat swarm, and Phasmatodea, respectively. In the literature, we can classify metaheuristic algorithms into four categories: swarm-intelligence-based approaches, bio-inspired algorithms, natural phenomena-based algorithms, and natural science-based algorithms. See Table 1 for algorithm details. Meanwhile, many improved strategies are applied to strengthen the optimization ability of metaheuristic algorithms, like multi-objective strategy [36-37], compact strategy [39], binary strategy [42], surrogate strategy [44] and so on. In addition, metaheuristics can be applied to a variety of domains, such as information hiding, wireless sensor network [45], etc.

In this paper, a metaheuristic optimization algorithm (SRO) based on natural phenomena is proposed. To evaluate the algorithm performance, we use the CEC2013 test suite, CEC2017 test suite and engineering cases as validation tools. The experimental results show that SRO is a metaheuristic optimization algorithm. In summary, the innovations of this paper are as follows.

1. A new optimization algorithm SRO based on natural phenomena is proposed, which can simulate the rescue behavior of a ship.
2. A series of experiments were applied on a new test function combined into CEC2013 and CEC2017 as well as on three practical engineering problems, and the consequences of these experiments laid the foundation for further research.

*Corresponding Author: Jeng-Shyang Pan; E-mail: jengshyangpan@gmail.com
DOI: 10.53106/160792642024012501006

3. The convergence ability of the algorithm in different dimensions is evaluated by comparing it with the currently widely used metaheuristic algorithm, and the superiority of the SRO algorithm is demonstrated for high-dimensional problems.
4. Compared with other competitive metaheuristic algorithms, SRO can avoid staying in local optima.

The rest of this paper is organized as follows. The detailed description of the SRO algorithm is given in Section 2. Section 3 evaluates the results of SRO based on the test suites. Section 4 discusses experiments on three real-world engineering problems. Section 5 makes a conclusion.

Table 1. A summary of particle algorithms

Classifications	Algorithms	Authors	Descriptions
Swarm-intelligence-based	GA [3]	Holland et al.	Crossover, Mutation, Selection
	DE [8-9]	Storn et al.	Population evolutionary model
	HS [19]	Geem et al.	Harmony memory
Bio-inspired	PSO [6]	Kennedy et al.	Behavior of particle swarms
	ACO [4]	Dorigo et al.	Behavior of the ant colony
	ABC [10-11]	Karaboga et al.	Behavior of bee colonies
	DEO [18]	Kaveh et al.	Behavior of the dolphin echolocation
	GWO [12-13]	Mirjalili et al.	Behavior of the wolves
	HHO [16]	Heidari et al.	Behavior of Harris Hawks
	STOA [17]	Ghiman et al.	Behavior of sea bird sooty tern
	CSO [15, 38, 43]	Chu et al.	Behavior of cat swarm
	PPE [46]	Song et al.	Behavior of Phasmatodea
Natural science-based	SA [20]	Metropolis et al.	Derived from the solid annealing principle
	GSA [21-22]	Rashedi et al.	The law of gravity and particle interactions
	BH [26]	Hatamlou et al.	Black hole phenomenon
	MVO [28]	Mirjalili et al.	Describe the multi-verse optimization
	IPO [25]	Mozaffari et al.	Based on the Newtons second law
	GSO [27]	Muthiah-Nakarajan et al.	Galactic motion
	HGSO [23]	Hashim et al.	Henry's law of gas solubility
	AOA [24]	Abualigah et al.	Archimedes principle
Natural phenomena-based	IWD [34]	Shah-Hosseini et al.	Observing natural water drops that flow in rivers
	TLBO [33]	Rao et al.	The traditional classroom teaching process
	WCA [32]	Eskander et al.	Describe the flow of streams, rivers and lakes
	BSA [30-31]	Civicioglu et al.	Describe the backtracking optimization
	VCS [29]	Li et al.	The virus infection and diffusion strategies
	QS [35]	Zhang et al.	Human activities in queuing

2 Ship Rescue Optimization (SRO)

In this section, the source of inspiration and introduction for the SRO algorithm are provided.

2.1 Inspiration (First-order Approximate Ship Maneuvering Law of Movement)

Ship maneuverability is one of the important hydrodynamic properties of a ship, and is closely related to the safety of ship navigation. With the growth of the maritime industry and the raising of people's safety consciousness, the maneuverability of the ship is getting more and more attention.

The ship motion process is approximated to derive the first-order approximate ship maneuvering law of motion (commonly referred to as the K T equation). The specific equation is shown in Equation (1).

$$T \cdot \frac{d\omega(t)}{dt} + \omega(t) = K \cdot \delta(t). \quad \textbf{(1)}$$

Where $\omega(t)$ denotes the ship's rotation angular velocity at t, T is the ship's followership coefficient, K is the ship's cyclotron coefficient, and $\delta(t)$ is the ship's rudder angle at t. Observe that this equation is a first-order linear differential equation. Therefore, dividing both sides equally by T, we get the Equation (2).

$$\frac{d\omega(t)}{dt} + \frac{1}{T} \cdot \omega(t) = \frac{K \cdot \delta(t)}{T}. \quad \textbf{(2)}$$

We can solve for Equation (2), the final general solution of this equation is obtained as Equation (3). The equation of the variation of the rotation angular velocity of the ship with time can be obtained, and then the maneuvering motion of the ship is simulated.

$$\omega(t) = C(t) \cdot e^{-\frac{t}{T}} + K \cdot \delta(t). \quad \textbf{(3)}$$

Among these, $\omega(t)$ denotes the ship's rotational angular velocity at t, T is the ship's followership coefficient, K is the ship's cyclotron coefficient, $\delta(t)$ is the ship's rudder angle at t, and $C(t)$ denotes the coefficient at t.

2.2 SRO Algorithm

Inspired by the first-order approximate ship maneuvering motion law and considering the natural phenomena in the ship rescue process, we then simulate the process of ship rescue. We can divide the ship rescue into two cases, one is delayed rescue, so we need to search a large area at a certain piece of search and rescue; the other is an immediate rescue, in which the specific or approximate location of the searched person has been until, and only a small range of timely search in the shortest possible time is required. We can map these two types of search and rescue as algorithmic exploration and exploitation processes, respectively. The specific procedure of the algorithm is as follows.

Step 1: Initialization.

The number of ships (population size N) and ship location initialization equations are given as Equation (4).

$$X_i(t+1) = X_{\min} + r \times (X_{\max} - X_{\min}). \tag{4}$$

Where t is the iteration time, r is a random number between 0 and 1. The position of a ship i at the tth iteration among all ships N is denoted by $X_i(t)$, $X_{\min}$ and $X_{\max}$ is the bound of the problem.

Step 2: Group the ships.

Dividing all ships into G groups averagely, the number of ships in each group is N/G. At this time, the position of each ship can be represented by X_i^g, $g \in \{1,...,G\}$, $i \in \{1,...,N/G\}$.

Step 3: Evaluate the optimal in each group and global optimal overall ships.

The optimal ship position of each group is defined as X_{best}^g, and the global optimal ship position of the whole ship is defined as X_{best}.

Step 4: Update the ship maneuvering function of movement.

From the ship maneuvering function of movement, we get Equation (3). We define the coefficient T as the maximum number of iterations Max_iter, which yields Equation (5).

$$w_i^g(t+1) = C_i^g(t) \cdot e^{-\frac{t}{Max\_iter}} + k \cdot \delta_i^g(t), \tag{5}$$

where t is the current number of iterations, Max_iter is the maximum number of iterations, and k is a regular constant. $C_i^g(t)$ is the constant of the gth group of ships i that changes with the number of iterations at the t iteration, the equation is given as Equation (6). $\omega_i^g(t)$ is the rotational angular velocity of the gth group of ships i at the tth iteration, and $\delta_i^g(t)$ denotes the rudder angle of the gth group of ships i at the tth iteration, and the equation is given as Equation (7).

$$C_i^g(t+1) = \frac{\omega_i^g(t) - k \cdot \delta_i^g(t)}{e^{\frac{-t}{Max\_iter}}}. \tag{6}$$

$$\delta_i^g(t+1) = c \cdot F \cdot angle_i^g(t). \tag{7}$$

In Equation (7), c is the random number with a range of $(-2, 2)$. F is the directional coefficient controlling the direction of rudder angle of ship motion with the value of 1 or -1, and $angle_i^g(t)$ is the angle value between two ships at the tth iteration for the gth group of ships, which is calculated as follows Equation (8).

$$angle_i^g(t) = arc\cos\frac{X_i^g(t) \cdot X_{best}^g}{\| X_i^g(t) \| \cdot \| X_{best}^g \|}. \tag{8}$$

The ship maneuvering schematic is shown in Figure 1.

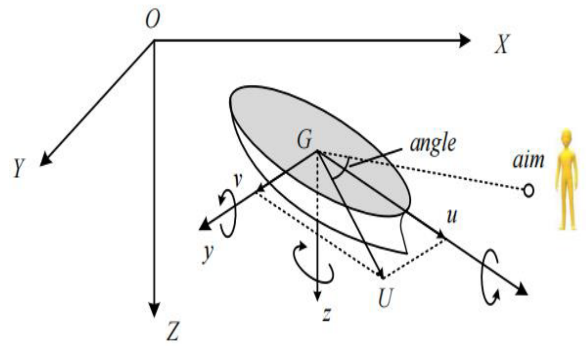

Figure 1. Ship maneuvering schematic

Step 5: Exploration phase.

If the optimal value does not change within 10 consecutive generations during the ship position update, the first stage update formula is executed to update the ship position, the update formula is shown in the Equation (9).

$$\begin{aligned} X_i^g(t+1) &= X_{best}^g(t) + c1 \cdot V_i^g(t) \cdot cos(D_i^g(t)) \\ &-c2 \cdot (X_{best}^g(t) - X_i^g(t)). \end{aligned} \tag{9}$$

To give more randomness into the algorithm, we give $c1$, $c2$ two coefficients, the range of $c1$ is (0, 1) and the range of $c2$ is $(-1, 1)$. $D_i^g(t)$ is the movement direction of the ship in the gth group of ships i at the tth iteration, and the range of this is $(-\pi, \pi)$. The specific calculation equation is as follows.

$$D_i^g(t+1) = D_i^g(t) + \delta_i^g(t). \tag{10}$$

$V_i^g(t)$ is the movement speed of the ship under the ith iteration of the gth group of ships i, and the initial value is 0, the formula use Equation (11).

$$V_i^g(t+1) = V_i^g(t) + a_i^g(t). \tag{11}$$

where $a_i^g(t)$ is the acceleration during the ship's motion, and the initial value is $1e-6$.

Step 6: Exploitation phase.

If there is any one generation change within 10 consecutive generations during the ship position update. The second stage motion formula is inspired by the motion trajectory of the ship during a small search. At this point, the ship's search trajectory can be classified into three types: spiral-based search, sector-based search, and inward-joining circle-based search.

Case 1: When the number of populations is $[1, \frac{1}{2}N]$, then the ship is based on a spiral search.

$$X_i^g(t+1) = X_i^g(t) + (S_1(t) + S_2(t)). \quad \textbf{(12)}$$

$$S_1(t) = m \cdot n(t) \cdot cos((X_i^g(t))) \cdot dist_a(t). \quad \textbf{(13)}$$

$$S_2(t) = m \cdot n(t) \cdot sin((X_i^g(t))) \cdot dist_b(t). \quad \textbf{(14)}$$

$$\begin{aligned} dist_a(t) &= X_{best}^g(t) - X_i^g(t). \\ dist_b(t) &= X_{best}(t) - X_i^g(t). \end{aligned} \quad \textbf{(15)}$$

$$n(t) = \frac{-t}{2\pi \cdot Max\_iter}. \quad \textbf{(16)}$$

where $S_1(t)$, $dist_a(t)$ represent the group optimal motion curve and the distance to the current position, respectively. $S_2(t)$, $dist_b(t)$ indicate the global optimal curve and the distance from the current position. m is a random number from −1 to 1.

Case 2: When the number of populations is $(\frac{1}{2}N, \frac{9}{10}N]$, then the ship is based on sector search.

$$X_i^g(t+1) = X_i^g(t) + \frac{\pi}{3} \cdot m \cdot dist_b(t) \cdot stepsize. \quad \textbf{(17)}$$

Where *stepsize* satisfies the Lévy flight motion with the following equation.

$$stepsize(dim) = 0.01 \times \frac{u \times \sigma}{|v|^{\frac{1}{\beta}}}. \quad \textbf{(18)}$$

$$\sigma = \left(\frac{\Gamma(1+\beta) \times sin(\frac{\pi\beta}{2})}{\Gamma\frac{1+\beta}{2} \times \beta \times 2^{(\frac{\beta-1}{2})}}\right)^{\frac{1}{\beta}}. \quad \textbf{(19)}$$

Where u, σ is a random number of (0, 1), $\beta = 1.5$.

Case 3: When the number of populations is $(\frac{9}{10}N, N]$, then the ship is based on circle search.

$$\begin{aligned} X_i^g(t+1) &= m \cdot Q(t) \cdot cos(X_i^g(t)) \\ &+ dist_a(t) \cdot cos(M(t)). \end{aligned} \quad \textbf{(20)}$$

Where the expression of $Q(t)$ and $M(t)$ are as follows:

$$Q(t) = dist_a(t) - dist_b(t). \quad \textbf{(21)}$$

$$M(t) = Q(t) \cdot X_i^g(t). \quad \textbf{(22)}$$

Similarly, m represents a random number in the range (−1, 1). The expression of $dist_a$, $dist_b$ is Equation (15).

Step 7: Ship squad communication.

Every 20 generations, the ships communicate with each other and update the worst 3 ship positions of each group using Equation (23).

$$\begin{aligned} X_i^g(t+1) &= X_i^g(t) + c_1 \cdot (X_{best}^g(t) - X_i^g(t)) \\ &+ c_2 \cdot (X_{best}(t) - X_i^g(t)). \end{aligned} \quad \textbf{(23)}$$

where, $c_1 \in (0,2)$ and $c_2 \in (0,2)$.

2.3 SRO Pseudo-algorithm

The algorithm firstly initializes the position of each ship and then divides the whole ship team into several ship squads. All members of each squad choose the exploration or exploitation process according to the change of the current best individual with the number of iterations, and when the optimal value is changed within 10 consecutive generations in the process of updating the ship position, the first stage formula is executed, otherwise, the second stage formula is executed. At the same time, every n generation the ships communicate with each other and exchange information until the best individual is found or the algorithm reaches the limit of the maximum number of iterations. The specific pseudo-algorithm flow is given in Algorithm 1.

3 Results and Discussion

In this section, to study the performance of the SRO algorithm, qualitative experiments, quantitative experiments are analyzed and compared, respectively. Among them, the qualitative experiments mainly include the average optimal value and standard deviation of the algorithm in 10, 30, and 50 dimensions. The quantitative experiments mainly include the convergence behavior analysis of the algorithms.

3.1 Parameter Settings

This experiment was performed on a Windows 10 home 64-bit Matlab 9.2 (R2020b) laptop with an Intel(R) Core(TM) i7-10750H@2.6 GHz CPU and 16.00 GB RAM. The number of total ships in the overall N is 80, the maximum number of iterations is 1000, and the number of dimensions is 10, 30 or 50. To perform statistical analysis, all algorithms were run 30 times independently. In addition, the initial value of parameter k is $2e-5$, and the initial value of parameter α is $1e-6$.

3.2 Benchmark Set and Compared Algorithms

The CEC2013 test suite has a total of 28 test functions. These include three types of functions: unimodal, basic multimodal, and combined functions. Similarly, the CEC2017 test suite has a total of 29. These functions include four types: unimodal, basic multimodal, hybrid, and composite functions. To analyze the performance of our proposed algorithm more comprehensively, we selected two test suites, CEC2013 and CEC2017, to test our algorithm. Details of the test form are shown in Table 2.

In order to evaluate the performance of the SRO algorithm, this paper compares the SRO algorithm with Particle Swarm Optimization (PSO), Butterfly Optimization, Algorithm (BOA) [41], Black-Hole (BH) [26], Gravitational Search Algorithm (GSA) [21], Aquila Optimization (AO) [7], Sine Cosine Algorithm (SCA) [40], Harris Hawks Optimization (HHO) [16], Sooty Tern Optimization Algorithm (STOA) [17] in 10, 30, and 50 dimensions, respectively. For the comparison, the evaluation criteria are the average optimal value (Mean) and standard deviation (Std) of 30 runs at the maximum number of iterations of 1000 iterations.

3.3 Statistical Results and Discussion

In this experiment, we tested our proposed algorithm on three dimensional spaces, including 10, 30 and 50 dimensions, respectively. Table 3 to Table 8 are the statistics for the 10, 30, 50 dimensional conditions. Among them, the bolded data part of the table indicates the average optimal value of the best algorithm compared with other algorithms under the current function. From the point of view of the average optimal value, among all the compared algorithms, 42 functions of SRO are optimal in 10 dimensions, 46 functions of SRO outperform other algorithms in 30 dimensions, and 52 functions of SRO perform significantly in 50 dimensions. From the perspective of the distribution of the average optimal values, our proposed algorithm performs better especially on hybrid or composite functions, and 28 out of 28 hybrid or composite functions perform well in all 50 dimensions, for example. From the perspective of dimensional distribution, the algorithm has a greater advantage in higher dimensions.

3.4 Convergence Behavior Analysis

To further validate the superiority of the proposed SRO algorithm compared to other algorithms, we further performed convergence tests on nine algorithms including SRO. Here, we choose the 50 dimensions as examples, and some of the experimental results in 50 dimensions are shown in Figure 2. Subplots (a) to (d) in Figure 2 show the convergence curves of the nine algorithms for the unimodal functions F1, F2, F4, and F5. It can be seen from these plots that the SRO algorithm converges faster than the other algorithms on the unimodal functions. From the convergence curves (e), (f), (g) of the multimodal functions F24, F25, F26, and (h), (i), (j) of the hybrid function F30, F32, F33, it can be seen that the SRO algorithm as a whole has a fast convergence speed and the best final convergence value. The SRO algorithm also shows strong convergence performance from the convergence curves (l), (m), (n), (o), and (p) of the composite functions F46, F47, and F54-F56.

In summary, compared with other algorithms, our proposed algorithm can jump out the local optimal solution after a certain number of iterations, and the method has stronger search capability compared with other algorithms.

Algorithm 1. Pseudo-code SRO algorithm

Initialization: number of ship N,
X_i ($i = 1, 2, \ldots, N$), $C(t)$, $\omega(t)$, $\delta(t)$, F,
$angle_i(t)$, $V(t)$, $D_i(t)$.
Divide the ships into G groups.
Evaluate each group g.
Get the best ship of each group X_{best}^{g} and the best ship X_{best} in all groups.
while $t \leq$ *maximum number of iterations* do
    if mod (t, 20) then
        Update the worst 3 ship of each group using Equation (23).
    end if
    if there have no change during 10 iterations then
        Update the $w_i^g(t+1)$ using Equation (5).
        Update $C_i^g(t+1)$ using Equation (6).
        Update $\delta_i^g(t)$ using Equation (7).
        Update $angle_i^g(t)$ using Equation (8).
        Update the position of all ship $X_i^g(t)$ using Equation (9).
        Update $D_i^g(t)$ using Equation (10).
        Update $V_i^g(t)$ using Equation (11).
    else
        if $1 \leq$ the current number of ship $\leq N/2$ then
            Update the position of ship X_i^g using Equation (12).
        else if $N/2 <$ the current number of ship $\leq 9/10\ N$ then
            Update the position of ship using Equation (17).
    else
            Update the position of ship using Equation (20).

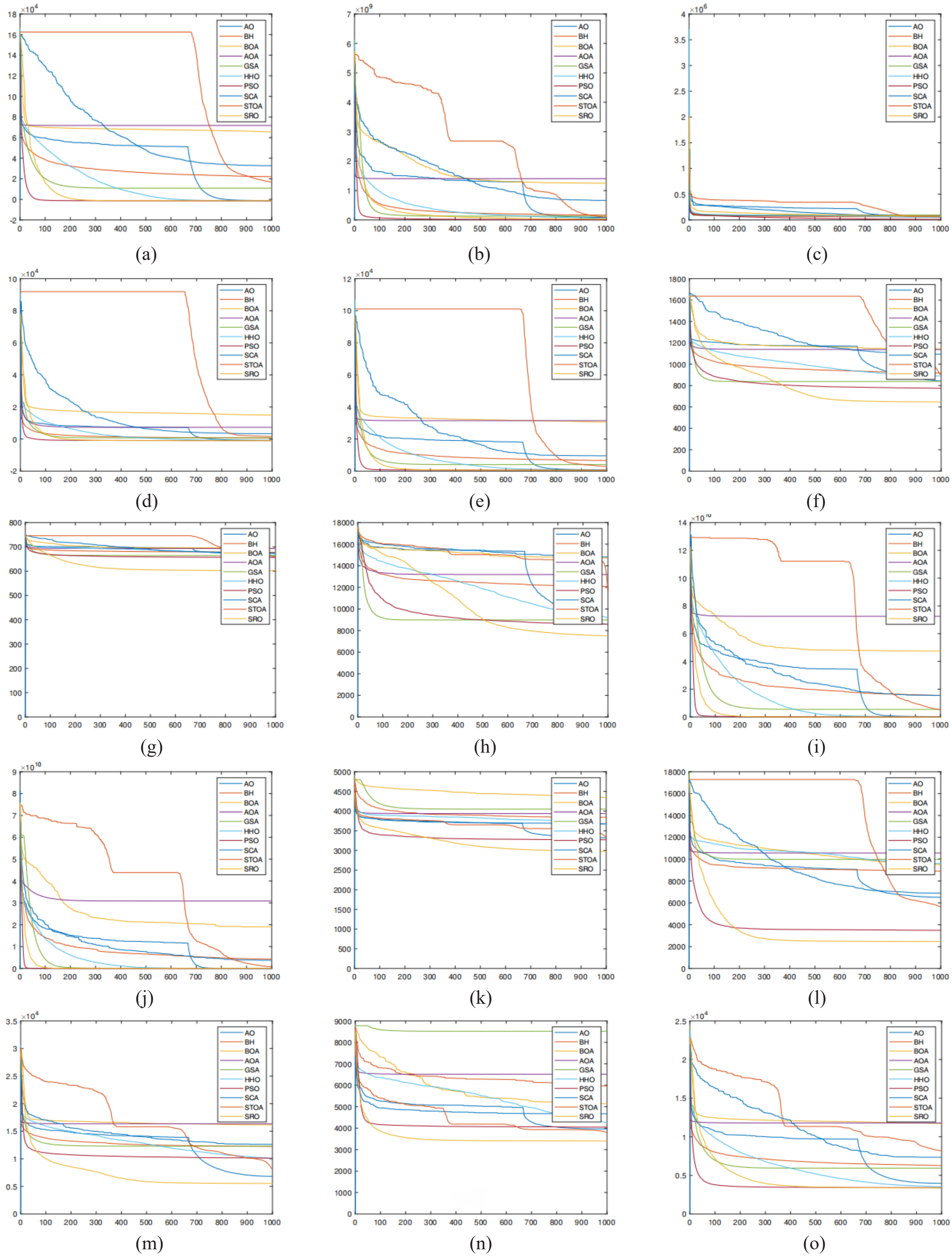

Figure 2. Convergence curves of competitive algorithms obtained on Dim = 50

Table 2. The test set used in this article

	No	ID	Description	$F^*_i = F_i(x^*)$
Unimodal functions	F1	CEC2013- No1	Sphere function	-1400
	F2	CEC2013- No2	Rotated high conditioned Elliptic function	-1300
	F3	CEC2013- No3	Rotated Bent Cigar function	-1200
	F4	CEC2013- No4	Rotated Discus function	-1100
	F5	CEC2013- No5	Different powers function	-1000
	F6	CEC2017- No1	Shifted and rotated Bent Cigar function	100
	F7	CEC2017- No2	Shifted and rotated Zakharov function	200
Basic multimodal functions	F8	CEC2013- No6	Rotated Rosenbrocks function	-900
	F9	CEC2013- No7	Rotated Schaffers F7 function	-800
	F10	CEC2013- No8	Rotated Ackleys function	-700
	F11	CEC2013- No9	Rotated Weierstrass function	-600
	F12	CEC2013- No10	Rotated Griewanks function	-500
	F13	CEC2013- No11	Rastrigins function	-400
	F14	CEC2013- No12	Rotated Rastrigins function	-300
	F15	CEC2013- No13	Non-continuous rotated Rastrigins function	-200
	F16	CEC2013- No14	Schwefel's function	-100
	F17	CEC2013- No15	Rotated Schwefel's function	100
	F18	CEC2013- No16	Rotated Katsuura function	200
	F19	CEC2013- No17	Lunacek Bi_Rastrigin function	300
	F20	CEC2013- No18	Rotated Lunacek Bi_Rastrigin function	400
	F21	CEC2013- No19	Expanded Griewanks plus Rosenbrocks function	500
	F22	CEC2013- No20	Expanded Scaffers F6 function	600
	F23	CEC2017- No3	Shifted and rotated Rosenbrocks function	300
	F24	CEC2017- No4	Shifted and rotated Rastrigins function	400
	F25	CEC2017- No5	Shifted and rotated expanded Scaffers F6 function	500
	F26	CEC2017- No6	Shifted and rotated Lunacek Bi_Rastrigin function	600
	F27	CEC2017- No7	Shifted and rotated non-continuous Rastrigins function	700
	F28	CEC2017- No8	Shifted and rotated Levy function	800
	F29	CEC2017- No9	Shifted and rotated Schwefels function	900
Hybrid functions	F30	CEC2017- No10	Hybrid function 1 (N = 3)	1000
	F31	CEC2017- No11	Hybrid function 2 (N = 3)	1100
	F32	CEC2017- No12	Hybrid function 3 (N = 3)	1200
	F33	CEC2017- No13	Hybrid function 4 (N = 4)	1300
	F34	CEC2017- No14	Hybrid function 5 (N = 4)	1400
	F35	CEC2017- No15	Hybrid function 6 (N = 4)	1500
	F36	CEC2017- No16	Hybrid function 6 (N = 5)	1600
	F37	CEC2017- No17	Hybrid function 6 (N = 5)	1700
	F38	CEC2017- No18	Hybrid function 6 (N = 5)	1800
	F39	CEC2017- No19	Hybrid function 6 (N = 6)	1900
Composition functions	F40	CEC2013- No21	Composition function 1 (n = 5, rotated)	700
	F41	CEC2013- No22	Composition function 2 (n = 3, unrotated)	800
	F42	CEC2013- No23	Composition function 3 (n = 3, rotated)	900
	F43	CEC2013- No24	Composition function 4 (n = 3, rotated)	1000
	F44	CEC2013- No25	Composition function 5 (n = 3, rotated)	1100
	F45	CEC2013- No26	Composition function 6 (n = 5, rotated)	1200
	F46	CEC2013- No27	Composition function 7 (n = 5, rotated)	1300
	F47	CEC2013- No28	Composition function 8 (n = 5, rotated)	1400
	F48	CEC2017- No20	Composition function 1 (N = 3)	2000
	F49	CEC2017- No21	Composition function 2 (N = 3)	2100
	F50	CEC2017- No22	Composition function 3 (N = 4)	2200
	F51	CEC2017- No23	Composition function 4 (N = 4)	2300
	F52	CEC2017- No24	Composition function 5 (N = 5)	2400
	F53	CEC2017- No25	Composition function 6 (N = 5)	2500
	F54	CEC2017- No26	Composition function 7 (N = 6)	2600
	F55	CEC2017- No27	Composition function 8 (N = 6)	2700
	F56	CEC2017- No28	Composition function 9 (N = 3)	2800
	F57	CEC2017- No29	Composition function 10 (N = 3)	2900

Table 3. Results of benchmark functions (F1-F29), with 10 dimensions

		SRO	PSO	BOA	BH	GSA	AO	SCA	HHO	STOA
F1	Mean	-1.40E+03	-1.40E+03	3.95E+03	-1.38E+03	-1.40E+03	-1.40E+03	-8.79E+02	-1.40E+03	-1.19E+03
	Std	1.05E-11	1.43E-03	1.15E+03	7.03E+00	0.00E+00	9.70E-02	1.81E+02	1.02E-01	1.77E+02
F2	Mean	1.48E+05	1.14E+05	4.56E+06	1.74E+06	4.75E+06	2.77E+06	4.61E+06	1.09E+06	1.64E+06
	Std	1.14E+05	1.99E+05	2.11E+06	2.88E+05	9.63E+05	1.83E+06	2.37E+06	8.92E+05	1.44E+06
F3	Mean	1.22E+07	7.04E+07	1.97E+10	5.02E+08	9.65E+08	2.57E+08	8.23E+08	3.36E+08	3.15E+08
	Std	2.13E+07	1.06E+08	8.43E+09	2.62E+08	8.39E+08	3.39E+08	7.37E+08	4.64E+08	3.80E+08
F4	Mean	1.11E+03	-1.01E+03	9.40E+03	4.54E+03	1.62E+04	7.05E+03	4.32E+03	5.04E+03	4.02E+03
	Std	1.77E+03	3.06E+01	2.80E+03	1.22E+03	1.70E+03	2.07E+03	2.09E+03	1.38E+03	2.58E+03
F5	Mean	-1.00E+03	-1.00E+03	4.03E+02	-9.83E+02	-1.00E+03	-9.99E+02	-8.56E+02	-1.00E+03	-9.35E+02
	Std	1.24E-06	6.73E-03	7.08E+02	3.63E+00	6.44E-05	6.66E-01	1.17E+02	7.20E-02	1.09E+02
F6	Mean	2.98E+03	5.09E+03	2.45E+09	1.32E+08	3.02E+02	2.57E+05	6.41E+08	2.70E+05	1.73E+08
	Std	2.63E+03	2.49E+03	1.08E+09	4.60E+07	2.08E+02	1.02E+05	2.13E+08	1.27E+05	2.39E+08
F7	Mean	3.00E+02	3.00E+02	5.86E+03	4.43E+02	1.08E+04	3.24E+02	1.33E+03	3.01E+02	7.93E+02
	Std	1.61E-03	8.12E-02	2.27E+03	5.57E+01	1.41E+03	2.81E+01	7.13E+02	5.22E-01	6.27E+02
F8	Mean	-8.92E+02	-8.91E+02	-4.51E+02	-8.29E+02	-8.30E+02	-8.68E+02	-8.63E+02	-8.49E+02	-8.64E+02
	Std	3.47E+00	2.48E+00	1.30E+02	1.84E+01	2.08E+00	3.27E+01	2.03E+01	3.54E+01	3.40E+01
F9	Mean	-7.89E+02	-7.66E+02	-6.67E+02	-7.59E+02	-7.64E+02	-7.55E+02	-7.58E+02	-7.15E+02	-7.72E+02
	Std	1.22E+01	2.02E+01	1.25E+02	2.11E+01	2.40E+01	1.44E+01	7.47E+00	2.89E+01	1.45E+01
F10	Mean	-6.80E+02	-6.80E+02	-6.80E+02	-6.80E+02	-6.80E+02	-6.80E+02	-6.80E+02	-6.80E+02	-6.80E+02
	Std	9.02E-02	4.06E-02	6.30E-02	7.10E-02	8.42E-02	6.80E-02	6.59E-02	7.50E-02	7.69E-02
F11	Mean	-5.96E+02	-5.94E+02	-5.93E+02	-5.93E+02	-5.95E+02	-5.94E+02	-5.92E+02	-5.93E+02	-5.93E+02
	Std	9.65E-01	1.51E+00	6.15E-01	1.16E+00	1.46E+00	1.44E+00	1.02E+00	1.51E+00	1.64E+00
F12	Mean	-5.00E+02	-5.00E+02	9.20E+01	-4.93E+02	-5.00E+02	-4.96E+02	-4.32E+02	-4.98E+02	-4.62E+02
	Std	1.59E-01	1.16E-01	1.96E+02	1.84E+00	1.11E-01	2.30E+00	2.32E+01	7.81E-01	3.36E+01
F13	Mean	-3.97E+02	-3.83E+02	-2.94E+02	-3.47E+02	-3.53E+02	-3.75E+02	-3.44E+02	-3.75E+02	-3.64E+02
	Std	1.41E+00	9.20E+00	2.06E+01	1.47E+01	8.01E+00	9.98E+00	7.10E+00	8.37E+00	1.45E+01
F14	Mean	-2.87E+02	-2.71E+02	-1.99E+02	-2.46E+02	-2.48E+02	-2.61E+02	-2.47E+02	-2.13E+02	-2.66E+02
	Std	5.14E+00	1.01E+01	1.66E+01	1.48E+01	7.67E+00	1.07E+01	6.57E+00	3.49E+01	9.81E+00
F15	Mean	-1.82E+02	-1.63E+02	-9.84E+01	-1.42E+02	-1.21E+02	-1.42E+02	-1.44E+02	-1.13E+02	-1.60E+02
	Std	7.64E+00	1.05E+01	1.71E+01	1.27E+01	1.22E+01	1.87E+01	9.96E+00	2.20E+01	1.08E+01
F16	Mean	7.64E+00	5.49E+02	1.58E+03	1.01E+03	9.58E+02	4.32E+02	1.17E+03	4.29E+02	8.65E+02
	Std	1.17E+02	1.62E+02	1.50E+02	2.05E+02	2.87E+02	2.47E+02	2.35E+02	2.88E+02	3.10E+02
F17	Mean	8.93E+02	8.67E+02	1.60E+03	9.58E+02	8.13E+02	7.18E+02	1.54E+03	9.73E+02	1.30E+03
	Std	3.20E+02	2.71E+02	1.33E+02	3.09E+02	3.09E+02	2.31E+02	1.82E+02	2.49E+02	3.67E+02
F18	Mean	2.01E+02	2.01E+02	2.01E+02	2.01E+02	2.00E+02	2.01E+02	2.01E+02	2.01E+02	2.01E+02
	Std	2.58E-01	2.08E-01	1.94E-01	1.85E-01	2.86E-02	2.83E-01	1.79E-01	2.21E-01	2.11E-01
F19	Mean	3.17E+02	3.33E+02	3.99E+02	3.54E+02	3.13E+02	3.54E+02	3.60E+02	3.90E+02	3.46E+02
	Std	3.20E+00	6.76E+00	1.25E+01	9.59E+00	1.17E+00	1.25E+01	7.62E+00	2.73E+01	9.24E+00
F20	Mean	4.26E+02	4.30E+02	5.02E+02	4.55E+02	4.12E+02	4.54E+02	4.66E+02	4.86E+02	4.54E+02
	Std	5.91E+00	3.97E+00	1.37E+01	9.12E+00	1.22E+00	9.67E+00	1.07E+01	2.48E+01	1.23E+01
F21	Mean	5.01E+02	5.01E+02	3.29E+03	5.07E+02	5.01E+02	5.04E+02	5.11E+02	5.07E+02	5.03E+02
	Std	2.10E-01	3.76E-01	2.53E+03	2.31E+00	3.86E-01	1.67E+00	1.38E+01	2.71E+00	7.58E-01
F22	Mean	6.03E+02	6.03E+02	6.04E+02	6.03E+02	6.04E+02	6.03E+02	6.04E+02	6.04E+02	6.03E+02
	Std	5.02E-01	3.84E-01	3.16E-01	4.35E-01	3.14E-01	3.83E-01	3.68E-01	4.34E-01	3.37E-01
F23	Mean	4.03E+02	4.04E+02	9.32E+02	4.15E+02	4.06E+02	4.08E+02	4.40E+02	4.12E+02	4.25E+02
	Std	1.20E+00	3.63E+00	2.07E+02	8.01E+00	1.03E+00	1.28E+01	1.75E+01	2.02E+01	2.25E+01
F24	Mean	5.08E+02	5.29E+02	5.71E+02	5.44E+02	5.60E+02	5.23E+02	5.47E+02	5.41E+02	5.24E+02
	Std	3.55E+00	1.37E+01	1.05E+01	1.20E+01	8.35E+00	8.24E+00	6.15E+00	1.91E+01	7.37E+00
F25	Mean	6.00E+02	6.08E+02	6.21E+02	6.26E+02	6.23E+02	6.14E+02	6.16E+02	6.30E+02	6.08E+02
	Std	3.81E-05	6.89E+00	6.09E+00	6.20E+00	8.64E+00	5.95E+00	2.86E+00	1.13E+01	4.26E+00
F26	Mean	7.19E+02	7.25E+02	7.85E+02	7.54E+02	7.14E+02	7.51E+02	7.74E+02	7.75E+02	7.51E+02
	Std	3.56E+00	6.66E+00	1.02E+01	1.40E+01	1.52E+00	1.43E+01	7.79E+00	2.04E+01	1.14E+01
F27	Mean	8.08E+02	8.15E+02	8.46E+02	8.27E+02	8.22E+02	8.23E+02	8.39E+02	8.29E+02	8.23E+02
	Std	3.67E+00	7.58E+00	5.29E+00	8.11E+00	3.88E+00	7.02E+00	6.41E+00	7.14E+00	5.73E+00
F28	Mean	9.00E+02	9.00E+02	1.11E+03	9.64E+02	9.00E+02	9.79E+02	9.78E+02	1.34E+03	9.63E+02
	Std	2.32E-10	5.67E-02	1.49E+02	4.51E+01	0.00E+00	5.11E+01	3.23E+01	2.10E+02	3.41E+01
F29	Mean	1.35E+03	2.01E+03	2.49E+03	2.04E+03	2.83E+03	1.79E+03	2.26E+03	1.94E+03	1.67E+03
	Std	1.45E+02	1.35E+02	1.59E+02	2.89E+02	3.03E+02	2.47E+02	2.06E+02	2.02E+02	2.00E+02

Table 4. Results of benchmark functions (F30-F57), with 10 dimensions

		SRO	PSO	BOA	BH	GSA	AO	SCA	HHO	STOA
F30	Mean	1.010E+03	1.13E+03	1.25E+03	1.14E+03	1.14E+03	1.16E+03	1.19E+03	1.17E+03	1.20E+03
	Std	2.47E+00	7.89E+00	6.51E+01	1.16E+01	2.05E+01	3.17E+01	2.95E+01	7.20E+01	7.85E+01
F31	Mean	1.42E+04	1.15E+04	5.72E+06	1.00E+06	7.27E+05	3.16E+06	1.11E+07	1.26E+06	2.03E+06
	Std	1.01E+04	9.83E+03	4.44E+06	4.86E+02	3.79E+05	3.06E+06	7.58E+06	1.54E+06	2.07E+06
F32	Mean	2.01E+03	1.07E+04	4.31E+04	1.34E+04	1.10E+04	1.09E+04	2.60E+04	1.44E+04	1.90E+04
	Std	1.70E+03	7.12E+03	3.01E+04	4.67E+03	1.42E+03	8.55E+03	1.50E+04	1.11E+04	1.97E+04
F33	Mean	1.43E+03	1.48E+03	2.48E+03	1.62E+03	6.21E+03	1.74E+03	1.59E+03	1.52E+03	1.56E+03
	Std	1.21E+01	2.55E+01	9.39E+02	2.21E+02	1.13E+03	3.19E+02	7.73E+01	3.20E+01	8.86E+01
F34	Mean	1.52E+03	1.78E+03	5.94E+03	3.66E+03	1.85E+04	3.27E+03	1.92E+03	2.19E+03	2.38E+03
	Std	1.29E+01	2.15E+02	2.98E+03	1.55E+03	4.29E+03	1.18E+03	2.18E+02	8.24E+02	8.39E+02
F35	Mean	1.61E+03	1.81E+03	1.85E+03	1.80E+03	2.13E+03	1.73E+03	1.70E+03	1.84E+03	1.74E+03
	Std	3.19E+01	1.09E+02	8.54E+01	1.21E+02	8.58E+01	1.08E+02	4.92E+01	1.33E+02	1.33E+02
F36	Mean	1.72E+03	1.75E+03	1.79E+03	1.77E+03	1.84E+03	1.76E+03	1.77E+03	1.77E+03	1.76E+03
	Std	1.13E+01	2.49E+01	1.67E+01	2.60E+01	9.68E+01	2.21E+01	1.58E+01	3.42E+01	3.57E+01
F37	Mean	4.10E+03	1.13E+04	2.04E+05	6.83E+03	9.29E+03	2.61E+04	8.66E+04	1.76E+04	3.31E+04
	Std	3.30E+03	4.35E+03	1.89E+05	3.57E+03	2.91E+03	1.21E+04	4.80E+04	1.39E+04	1.61E+04
F38	Mean	1.91E+03	1.98E+03	1.69E+04	4.53E+03	5.79E+04	4.78E+03	4.40E+03	9.69E+03	6.13E+03
	Std	6.79E+00	8.67E+01	1.29E+04	1.85E+03	2.47E+04	4.22E+03	3.75E+03	8.24E+03	6.14E+03
F39	Mean	2.00E+03	2.11E+03	2.14E+03	2.08E+03	2.28E+03	2.09E+03	2.09E+03	2.12E+03	2.09E+03
	Std	5.05E+00	6.57E+01	2.60E+01	3.61E+01	7.17E+01	4.30E+01	1.37E+01	5.97E+01	5.67E+01
F40	Mean	1.08E+03	1.07E+03	1.22E+03	1.10E+03	1.10E+03	1.10E+03	1.11E+03	1.10E+03	1.09E+03
	Std	6.37E+01	9.00E+01	5.89E+01	6.04E-03	4.55E-13	3.48E-03	1.15E+01	5.20E-03	4.48E+01
F41	Mean	1.01E+03	1.78E+03	2.66E+03	2.19E+03	3.01E+03	1.69E+03	2.34E+03	1.71E+03	1.81E+03
	Std	1.18E+02	2.69E+02	1.65E+02	3.19E+02	2.42E+02	2.61E+02	1.77E+02	3.31E+02	2.66E+02
F42	Mean	1.85E+03	2.09E+03	2.72E+03	2.34E+03	2.40E+03	2.23E+03	2.60E+03	2.44E+03	2.04E+03
	Std	3.03E+02	3.31E+02	2.36E+02	2.85E+02	2.73E+02	2.94E+02	1.80E+02	3.54E+02	3.64E+02
F43	Mean	1.21E+03	1.22E+03	1.16E+03	1.20E+03	1.23E+03	1.22E+03	1.23E+03	1.23E+03	1.22E+03
	Std	3.80E+00	6.82E+00	8.36E+00	3.82E+01	4.27E+00	1.30E+01	1.91E+00	1.05E+01	4.44E+00
F44	Mean	1.30E+03	1.32E+03	1.26E+03	1.29E+03	1.32E+03	1.31E+03	1.33E+03	1.33E+03	1.32E+03
	Std	2.78E+01	1.66E+01	1.05E+01	3.48E+01	3.01E+00	2.20E+01	2.62E+00	4.07E+00	2.27E+00
F45	Mean	1.37E+03	1.39E+03	1.36E+03	1.36E+03	1.49E+03	1.39E+03	1.40E+03	1.45E+03	1.40E+03
	Std	4.05E+01	6.88E+01	8.93E+00	1.83E+01	4.54E+01	2.45E+01	3.66E-01	7.06E+01	3.79E-01
F46	Mean	1.74E+03	1.74E+03	1.85E+03	1.71E+03	1.70E+03	1.80E+03	1.91E+03	1.92E+03	1.86E+03
	Std	9.97E+01	1.14E+02	4.95E+01	1.91E+01	3.60E-10	8.61E+01	2.53E+01	1.02E+02	2.78E+01
F47	Mean	1.70E+03	1.99E+03	1.87E+03	2.06E+03	2.71E+03	2.05E+03	2.08E+03	2.24E+03	1.95E+03
	Std	7.24E+01	1.89E+02	2.54E+02	1.96E+02	8.21E+01	1.57E+02	9.53E+01	2.11E+02	1.42E+02
F48	Mean	2.26E+03	2.29E+03	2.21E+03	2.21E+03	2.36E+03	2.28E+03	2.23E+03	2.30E+03	2.20E+03
	Std	5.49E+01	6.24E+01	1.13E+01	1.55E+00	2.43E+01	5.67E+01	4.84E+01	6.52E+01	1.25E+00
F49	Mean	2.30E+03	2.36E+03	2.32E+03	2.32E+03	2.30E+03	2.31E+03	2.36E+03	2.31E+03	2.50E+03
	Std	1.44E+01	2.07E+02	1.67E+01	4.56E+00	4.12E-11	1.20E+01	3.34E+01	5.90E+00	4.12E+02
F50	Mean	2.61E+03	2.66E+03	2.64E+03	2.64E+03	2.76E+03	2.64E+03	2.65E+03	2.66E+03	2.63E+03
	Std	4.01E+00	2.16E+01	5.77E+01	1.05E+02	6.02E+01	1.42E+01	4.98E+00	2.78E+01	8.30E+00
F51	Mean	2.70E+03	2.75E+03	2.56E+03	2.56E+03	2.53E+03	2.75E+03	2.76E+03	2.77E+03	2.75E+03
	Std	9.14E+01	7.14E+01	1.60E+01	1.19E+02	9.87E+01	6.68E+01	7.20E+01	9.95E+01	1.28E+01
F52	Mean	2.92E+03	2.92E+03	3.25E+03	2.94E+03	2.94E+03	2.93E+03	2.96E+03	2.91E+03	2.94E+03
	Std	2.31E+01	2.20E+01	9.06E+01	1.82E+01	7.89E+00	2.28E+01	1.19E+01	8.55E+01	1.37E+01
F53	Mean	2.92E+03	2.95E+03	2.98E+03	2.98E+03	3.71E+03	2.95E+03	3.07E+03	3.50E+03	3.11E+03
	Std	4.44E+01	7.32E+01	6.89E+01	1.70E+02	6.15E+02	1.75E+02	5.01E+01	5.49E+02	3.27E+02
F54	Mean	3.09E+03	3.12E+03	3.11E+03	3.15E+03	3.26E+03	3.10E+03	3.10E+03	3.13E+03	3.09E+03
	Std	1.42E+00	3.67E+01	1.00E+01	1.52E+01	3.31E+01	3.80E+00	1.65E+00	3.62E+01	2.40E+00
F55	Mean	3.20E+03	3.22E+03	3.46E+03	3.16E+03	3.45E+03	3.34E+03	3.25E+03	3.30E+03	3.24E+03
	Std	1.40E+02	1.48E+02	2.30E+02	6.49E+01	2.61E+01	1.01E+02	4.08E+01	1.22E+02	8.56E+01
F56	Mean	3.16E+03	3.23E+03	3.28E+03	3.24E+03	3.43E+03	3.22E+03	3.22E+03	3.31E+03	3.17E+03
	Std	2.77E+01	7.20E+01	3.83E+01	3.35E+01	1.11E+02	4.55E+01	2.45E+01	9.80E+01	3.81E+01
F57	Mean	2.38E+05	2.71E+05	1.19E+06	8.16E+05	1.13E+06	2.56E+05	7.90E+05	8.70E+05	8.17E+04
	Std	3.91E+05	5.11E+05	1.04E+06	9.81E+05	3.76E+05	5.60E+05	5.59E+05	1.21E+06	1.45E+05

Table 5. Results of benchmark functions (F1-F29), with 30 dimensions

		ARO	PSO	BOA	BH	GSA	AO	SCA	HHO	STOA
F1	AVG	-1.40E+03	-1.37E+03	4.25E+04	1.04E+04	-9.26E+02	-1.38E+03	1.32E+04	1.32E+04	3.62E+03
	STD	1.19E-05	1.59E+02	4.18E+03	9.34E+02	3.85E+02	9.12E+00	3.15E+03	3.15E+03	2.17E+03
F2	AVG	8.88E+06	4.17E+06	4.32E+08	7.33E+07	3.52E+07	5.01E+07	2.01E+08	2.01E+08	4.18E+07
	STD	3.49E+06	1.03E+06	1.76E+08	6.89E+06	5.50E+06	1.82E+07	6.18E+07	6.18E+07	1.82E+07
F3	AVG	8.17E+08	2.72E+09	1.49E+18	1.81E+11	1.47E+12	2.16E+10	5.01E+10	5.01E+10	1.43E+10
	STD	8.96E+08	2.55E+09	5.31E+18	1.29E+11	2.68E+12	9.78E+09	2.06E+10	2.06E+10	5.82E+09
F4	AVG	3.56E+04	3.24E+03	4.87E+04	3.95E+04	6.93E+04	3.85E+04	4.34E+04	4.34E+04	3.69E+04
	STD	9.61E+03	1.06E+03	6.39E+03	4.23E+03	4.63E+03	4.14E+03	6.53E+03	6.53E+03	7.68E+03
F5	AVG	-1.00E+03	-9.56E+02	1.68E+04	5.61E+02	1.21E+02	-8.40E+02	1.94E+03	1.94E+03	6.28E+02
	STD	7.90E-03	4.94E+01	5.40E+03	1.78E+02	1.41E+02	4.64E+01	1.03E+03	1.03E+03	6.81E+02
F6	AVG	4.44E+03	1.57E+06	3.44E+10	8.30E+09	1.80E+08	3.07E+07	1.43E+10	1.31E+07	8.30E+09
	STD	4.00E+03	4.58E+05	5.23E+09	9.33E+08	1.98E+08	1.21E+07	2.32E+09	2.67E+06	2.50E+09
F7	AVG	3.21E+04	1.13E+03	5.73E+04	3.12E+04	2.70E+38	2.00E+27	1.18E+36	1.64E+04	4.08E+04
	STD	9.91E+03	5.78E+02	9.65E+03	2.22E+03	4.48E+38	4.73E+27	3.90E+36	5.09E+03	8.71E+03
F8	AVG	-8.53E+02	-8.26E+02	8.53E+03	4.24E+02	-5.82E+02	-7.53E+02	8.21E+01	8.21E+01	-6.35E+02
	STD	2.24E+01	2.19E+01	1.58E+03	1.24E+02	3.21E+02	3.79E+01	2.85E+02	2.85E+02	8.28E+01
F9	AVG	-7.33E+02	-6.68E+02	7.70E+04	7.28E+02	1.65E+04	-5.52E+02	-5.73E+02	-5.73E+02	-6.92E+02
	STD	1.75E+01	3.48E+01	1.12E+05	1.30E+03	1.95E+04	1.20E+02	4.33E+01	4.33E+01	2.47E+01
F10	AVG	-6.79E+02	-6.79E+02	-6.79E+02	-6.79E+02	-6.79E+02	-6.79E+02	-6.79E+02	-6.79E+02	-6.79E+02
	STD	5.42E-02	5.82E-02	4.25E-02	5.65E-02	6.19E-02	5.96E-02	4.70E-02	4.70E-02	5.44E-02
F11	AVG	-5.75E+02	-5.69E+02	-5.63E+02	-5.61E+02	-5.61E+02	-5.65E+02	-5.59E+02	-5.59E+02	-5.68E+02
	STD	3.29E+00	4.43E+00	1.47E+00	2.41E+00	2.89E+00	3.53E+00	1.42E+00	1.42E+00	3.62E+00
F12	AVG	-4.96E+02	-4.25E+02	6.38E+03	1.05E+03	-5.35E+01	-3.37E+02	1.51E+03	1.51E+03	3.04E+02
	STD	1.38E+00	4.61E+01	1.23E+03	1.32E+02	1.30E+02	4.95E+01	4.58E+02	4.58E+02	3.16E+02
F13	AVG	-3.57E+02	-1.72E+02	3.41E+02	7.10E+01	5.27E+01	-1.40E+02	2.64E-01	2.64E-01	-1.24E+02
	STD	1.03E+01	2.51E+01	6.81E+01	7.79E+01	3.83E+01	4.28E+01	3.70E+01	3.70E+01	4.47E+01
F14	AVG	-2.10E+02	-4.21E+01	4.20E+02	1.95E+02	2.60E+02	1.26E+01	1.00E+02	1.00E+02	-3.94E+01
	STD	3.32E+01	7.95E+01	5.83E+01	7.71E+01	5.92E+01	4.02E+01	3.84E+01	3.84E+01	2.87E+01
F15	AVG	-3.93E+01	9.59E+01	5.11E+02	3.06E+02	4.81E+02	2.11E+02	2.13E+02	2.13E+02	1.08E+02
	STD	2.42E+01	4.74E+01	6.05E+01	6.45E+01	5.89E+01	5.80E+01	3.33E+01	3.33E+01	5.09E+01
F16	AVG	1.42E+03	3.69E+03	7.81E+03	6.32E+03	4.30E+03	3.84E+03	7.31E+03	7.31E+03	5.23E+03
	STD	4.34E+02	4.26E+02	2.66E+02	9.31E+02	6.05E+02	7.63E+02	3.76E+02	3.76E+02	6.22E+02
F17	AVG	4.54E+03	4.38E+03	7.88E+03	6.20E+03	4.05E+03	4.82E+03	7.68E+03	7.68E+03	6.47E+03
	STD	5.80E+02	5.46E+02	2.58E+02	9.15E+02	4.70E+02	8.20E+02	2.99E+02	2.99E+02	8.50E+02
F18	AVG	2.02E+02	2.03E+02	2.03E+02	2.02E+02	2.00E+02	2.02E+02	2.03E+02	2.03E+02	2.03E+02
	STD	6.02E-01	3.90E-01	3.80E-01	4.51E-01	1.29E-02	3.48E-01	3.41E-01	3.41E-01	2.82E-01
F19	AVG	4.04E+02	5.61E+02	1.08E+03	7.71E+02	5.66E+02	7.53E+02	8.52E+02	8.52E+02	7.28E+02
	STD	2.10E+01	3.93E+01	6.08E+01	4.76E+01	3.33E+01	6.69E+01	5.45E+01	5.45E+01	5.05E+01
F20	AVG	5.73E+02	6.51E+02	1.16E+03	8.84E+02	6.57E+02	8.47E+02	9.55E+02	9.55E+02	8.55E+02
	STD	3.32E+01	3.09E+01	5.10E+01	6.54E+01	2.52E+01	6.41E+01	5.76E+01	5.76E+01	5.74E+01
F21	AVG	5.06E+02	5.15E+02	2.68E+05	3.76E+03	1.49E+03	5.42E+02	9.21E+03	9.21E+03	1.66E+03
	STD	1.87E+00	2.69E+00	9.15E+04	6.12E+02	3.16E+02	1.05E+01	1.27E+04	1.27E+04	1.63E+03
F22	AVG	6.12E+02	6.15E+02	6.15E+02	6.15E+02	6.15E+02	6.15E+02	6.14E+02	6.14E+02	6.14E+02
	STD	3.48E-01	2.63E-01	9.40E-02	1.97E-01	1.05E-02	4.38E-01	4.15E-01	4.15E-01	5.26E-01
F23	AVG	5.06E+02	5.04E+02	1.49E+04	2.15E+03	9.05E+04	3.25E+04	5.32E+04	5.41E+02	7.39E+02
	STD	1.89E+01	2.22E+01	2.62E+03	1.39E+02	6.48E+03	5.15E+03	9.79E+03	3.03E+01	9.44E+01
F24	AVG	5.78E+02	6.68E+02	8.74E+02	7.36E+02	7.14E+02	5.57E+02	1.88E+03	7.41E+02	6.82E+02
	STD	2.78E+01	1.72E+01	2.37E+01	3.44E+01	8.79E+01	2.57E+01	4.54E+02	2.38E+01	3.30E+01
F25	AVG	6.00E+02	6.47E+02	6.74E+02	6.66E+02	7.44E+02	6.79E+02	7.99E+02	6.61E+02	6.38E+02
	STD	4.86E-02	5.78E+00	6.62E+00	7.55E+00	1.42E+01	3.12E+01	1.88E+01	7.66E+00	5.79E+00
F26	AVG	8.10E+02	8.85E+02	1.33E+03	1.13E+03	6.58E+02	6.46E+02	6.55E+02	1.26E+03	1.04E+03
	STD	1.81E+01	3.09E+01	4.24E+01	8.49E+01	2.21E+00	8.02E+00	4.58E+00	7.22E+01	3.88E+01
F27	AVG	8.72E+02	9.12E+02	1.11E+03	9.79E+02	9.49E+02	1.03E+03	1.16E+03	9.63E+02	9.62E+02
	STD	2.00E+01	1.50E+01	1.71E+01	4.31E+01	3.06E+01	4.88E+01	4.42E+01	2.17E+01	2.31E+01
F28	AVG	9.61E+02	4.41E+03	9.15E+03	6.44E+03	4.32E+03	5.27E+03	6.33E+03	7.03E+03	4.27E+03
	STD	8.23E+01	9.47E+02	1.16E+03	1.50E+03	4.17E+02	9.54E+02	1.38E+03	5.82E+02	8.03E+02
F29	AVG	4.38E+03	5.22E+03	8.68E+03	7.15E+03	5.08E+03	5.13E+03	8.43E+03	5.63E+03	6.47E+03
	STD	5.35E+02	4.16E+02	2.43E+02	1.05E+03	4.68E+02	4.92E+02	4.01E+02	6.98E+02	7.24E+02

Table 6. Results of benchmark functions (F30-F57), with 30 dimensions

		ARO	PSO	BOA	BH	GSA	AO	SCA	HHO	STOA
F30	AVG	1.17E+03	1.26E+03	4.92E+03	1.59E+03	4.88E+03	1.57E+03	2.64E+03	1.25E+03	2.03E+03
	STD	3.24E+01	4.36E+01	1.07E+03	4.06E+01	8.10E+02	1.56E+02	5.31E+02	3.89E+01	6.74E+02
F31	AVG	3.69E+05	2.81E+06	5.12E+09	1.18E+09	7.59E+07	3.34E+07	1.66E+09	1.32E+07	3.91E+08
	STD	3.57E+05	1.39E+06	1.97E+09	1.36E+08	6.47E+07	1.99E+07	4.36E+08	8.98E+06	2.03E+08
F32	AVG	1.78E+04	5.81E+04	3.38E+09	8.82E+07	3.20E+04	4.41E+05	6.40E+08	5.25E+05	1.23E+08
	STD	1.77E+04	2.38E+04	2.21E+09	5.01E+07	7.36E+03	3.14E+05	2.58E+08	7.17E+05	1.09E+08
F33	AVG	1.01E+04	2.43E+04	4.09E+05	1.15E+05	1.08E+06	4.45E+05	2.89E+05	1.69E+05	1.32E+05
	STD	8.61E+03	6.69E+04	3.36E+05	3.25E+04	2.06E+05	4.85E+05	2.18E+05	1.63E+05	8.10E+04
F34	AVG	6.80E+03	1.60E+04	1.31E+07	3.65E+04	1.44E+04	9.73E+04	2.42E+07	5.82E+04	8.50E+06
	STD	5.17E+03	5.96E+03	1.11E+07	1.02E+04	2.32E+03	4.65E+04	1.86E+07	3.65E+04	1.56E+07
F35	AVG	2.30E+03	2.60E+03	5.63E+03	3.99E+03	3.64E+03	3.17E+03	3.83E+03	3.26E+03	3.01E+03
	STD	2.12E+02	3.07E+02	9.70E+02	3.05E+02	3.72E+02	4.21E+02	2.39E+02	3.23E+02	3.57E+02
F36	AVG	1.97E+03	2.24E+03	3.61E+03	2.54E+03	2.94E+03	2.26E+03	2.60E+03	2.51E+03	2.25E+03
	STD	1.37E+02	2.00E+02	3.97E+02	2.18E+02	1.86E+02	2.42E+02	1.84E+02	3.08E+02	1.91E+02
F37	AVG	3.56E+05	1.34E+05	5.94E+06	3.19E+05	4.97E+05	2.11E+06	5.94E+06	1.22E+06	1.07E+06
	STD	3.83E+05	7.06E+04	4.95E+06	1.45E+05	2.75E+05	1.70E+06	3.92E+06	1.41E+06	1.32E+06
F38	AVG	1.13E+04	1.50E+04	4.32E+07	1.07E+06	2.28E+05	7.74E+05	4.39E+07	3.51E+05	6.61E+06
	STD	1.20E+04	1.01E+04	6.38E+07	4.63E+05	8.86E+04	5.30E+05	2.49E+07	2.36E+05	9.01E+06
F39	AVG	2.29E+03	2.64E+03	2.87E+03	2.59E+03	3.00E+03	2.54E+03	2.75E+03	2.81E+03	2.63E+03
	STD	1.27E+02	1.57E+02	1.27E+02	1.84E+02	1.99E+02	1.88E+02	1.03E+02	1.62E+02	1.80E+02
F40	AVG	9.68E+02	1.09E+03	3.12E+03	2.19E+03	2.10E+03	1.14E+03	2.76E+03	2.76E+03	2.31E+03
	STD	8.37E+01	9.37E+01	5.17E+01	6.25E+01	2.21E+02	3.15E+01	1.29E+02	1.29E+02	3.23E+02
F41	AVG	2.41E+03	5.59E+03	9.16E+03	8.13E+03	7.73E+03	5.28E+03	8.67E+03	8.67E+03	6.73E+03
	STD	4.08E+02	8.88E+02	3.06E+02	5.55E+02	4.97E+02	7.95E+02	4.93E+02	4.93E+02	6.76E+02
F42	AVG	5.73E+03	6.15E+03	9.33E+03	8.54E+03	7.32E+03	7.01E+03	9.11E+03	9.11E+03	7.19E+03
	STD	8.54E+02	9.75E+02	2.33E+02	6.12E+02	2.98E+02	8.31E+02	3.96E+02	3.96E+02	9.71E+02
F43	AVG	1.27E+03	1.30E+03	1.33E+03	1.35E+03	1.48E+03	1.30E+03	1.32E+03	1.32E+03	1.29E+03
	STD	1.03E+01	1.37E+01	1.90E+01	1.26E+01	4.58E+01	7.25E+00	6.09E+00	6.09E+00	9.87E+00
F44	AVG	1.38E+03	1.43E+03	1.43E+03	1.48E+03	1.52E+03	1.42E+03	1.43E+03	1.43E+03	1.40E+03
	STD	1.03E+01	1.40E+01	1.14E+01	9.57E+00	1.09E+01	9.01E+00	4.31E+00	4.31E+00	1.05E+01
F45	AVG	1.42E+03	1.51E+03	1.41E+03	1.40E+03	1.59E+03	1.47E+03	1.42E+03	1.42E+03	1.44E+03
	STD	4.71E+01	8.37E+01	4.17E+00	3.91E-01	2.65E+01	9.05E+01	3.51E+01	3.51E+01	7.79E+01
F46	AVG	2.25E+03	2.47E+03	2.90E+03	2.66E+03	2.55E+03	2.53E+03	2.71E+03	2.71E+03	2.45E+03
	STD	1.11E+02	1.15E+02	6.90E+01	7.08E+01	7.76E+01	8.37E+01	4.17E+01	4.17E+01	1.12E+02
F47	AVG	1.74E+03	3.74E+03	5.96E+03	5.38E+03	5.84E+03	4.65E+03	4.25E+03	4.25E+03	3.37E+03
	STD	2.09E+02	1.22E+03	6.45E+02	3.62E+02	2.91E+02	3.58E+02	1.98E+02	1.98E+02	4.10E+02
F48	AVG	2.37E+03	2.48E+03	2.38E+03	2.56E+03	2.64E+03	2.46E+03	2.58E+03	2.56E+03	2.48E+03
	STD	1.47E+01	3.53E+01	7.75E+01	2.95E+01	3.76E+01	3.80E+01	2.61E+01	5.05E+01	2.70E+01
F49	AVG	3.67E+03	4.04E+03	3.57E+03	5.65E+03	7.31E+03	2.34E+03	9.02E+03	6.55E+03	7.95E+03
	STD	1.84E+03	1.94E+03	3.37E+02	1.53E+03	3.58E+02	2.03E+01	1.98E+03	1.82E+03	6.86E+02
F50	AVG	2.73E+03	3.03E+03	3.14E+03	3.29E+03	3.82E+03	2.90E+03	3.03E+03	3.13E+03	2.82E+03
	STD	2.17E+01	8.81E+01	8.87E+01	8.61E+01	1.28E+02	6.21E+01	2.96E+01	1.31E+02	2.90E+01
F51	AVG	2.90E+03	3.19E+03	3.67E+03	3.52E+03	3.55E+03	3.07E+03	3.19E+03	3.39E+03	2.97E+03
	STD	2.21E+01	9.48E+01	2.39E+02	6.84E+01	8.12E+01	5.97E+01	3.09E+01	1.18E+02	2.62E+01
F52	AVG	2.89E+03	2.91E+03	4.87E+03	3.10E+03	3.01E+03	2.93E+03	3.32E+03	2.92E+03	3.11E+03
	STD	9.01E+00	1.80E+01	3.32E+02	1.01E+01	1.36E+01	2.34E+01	1.62E+02	1.86E+01	7.53E+01
F53	AVG	4.49E+03	5.26E+03	9.74E+03	7.81E+03	7.96E+03	4.59E+03	7.35E+03	7.13E+03	5.48E+03
	STD	3.92E+02	2.05E+03	7.91E+02	8.34E+02	3.50E+02	1.44E+03	3.51E+02	1.30E+03	3.66E+02
F54	AVG	3.22E+03	3.38E+03	3.70E+03	3.99E+03	5.19E+03	3.31E+03	3.46E+03	3.40E+03	3.28E+03
	STD	1.57E+01	1.69E+02	2.02E+02	1.01E+02	3.32E+02	3.70E+01	5.31E+01	1.08E+02	3.60E+01
F55	AVG	3.24E+03	3.26E+03	6.88E+03	3.84E+03	3.53E+03	3.34E+03	4.05E+03	3.29E+03	5.22E+03
	STD	3.73E+01	3.06E+01	5.46E+02	5.11E+01	9.81E+01	2.98E+01	1.65E+02	2.59E+01	1.36E+03
F56	AVG	3.62E+03	4.18E+03	6.68E+03	5.17E+03	5.43E+03	4.38E+03	4.91E+03	4.44E+03	4.24E+03
	STD	1.49E+02	2.62E+02	1.06E+03	3.20E+02	2.48E+02	2.73E+02	2.26E+02	2.70E+02	2.33E+02
F57	AVG	1.15E+04	2.16E+05	2.67E+08	9.51E+06	3.63E+06	6.87E+06	1.09E+08	2.46E+06	2.13E+07
	STD	4.61E+03	1.23E+05	2.36E+08	1.25E+06	8.26E+05	5.57E+06	5.22E+07	1.32E+06	1.60E+07

Table 7. Results of benchmark functions (F1-F29), with 50 dimensions

		SRO	PSO	BOA	BH	GSA	AO	SCA	HHO	STOA
F1	Mean	-1.40E+03	-1.33E+03	6.65E+04	2.20E+04	1.08E+04	-1.20E+03	3.19E+04	-1.35E+03	1.70E+04
	Std	9.17E+02	1.87E+02	3.99E+03	1.35E+03	1.67E+03	7.97E+01	4.57E+03	1.01E+01	3.93E+03
F2	Mean	3.10E+07	1.30E+07	1.21E+09	1.58E+08	1.22E+08	9.47E+07	6.72E+08	5.50E+07	9.41E+07
	Std	1.16E+07	4.98E+06	3.30E+08	1.75E+07	3.53E+07	3.27E+07	1.92E+08	1.10E+07	3.14E+07
F3	Mean	8.49E+09	5.99E+09	1.52E+18	3.95E+10	2.73E+11	3.94E+10	1.29E+11	1.71E+10	4.21E+10
	Std	6.81E+09	7.06E+09	5.66E+18	2.95E+09	1.59E+11	1.16E+10	3.08E+10	7.62E+09	1.01E+10
F4	Mean	7.32E+04	1.19E+04	8.82E+04	5.73E+04	9.07E+04	8.76E+04	8.05E+04	4.61E+04	6.06E+04
	Std	1.54E+04	3.58E+03	8.12E+03	4.13E+03	4.85E+03	8.97E+03	1.07E+04	5.84E+03	6.22E+03
F5	Mean	-9.99E+02	-8.93E+02	1.53E+04	6.65E+02	7.11E+02	-7.07E+02	3.34E+03	-9.36E+02	1.63E+03
	Std	2.99E-01	2.65E+02	2.29E+03	9.37E+01	1.91E+02	7.42E+01	2.28E+03	2.00E+01	1.27E+03
F6	Mean	7.92E+05	2.88E+08	8.01E+10	3.28E+10	2.01E+10	5.35E+08	5.02E+10	8.14E+07	3.07E+10
	Std	3.52E+05	4.60E+08	8.35E+09	1.58E+09	1.93E+09	2.10E+08	5.18E+09	1.42E+07	8.15E+09
F7	Mean	1.51E+05	1.83E+04	2.15E+05	1.03E+05	1.85E+05	1.77E+05	1.45E+05	6.50E+04	1.04E+05
	Std	2.89E+04	4.75E+03	2.74E+04	6.18E+03	1.06E+04	1.72E+04	1.86E+04	1.07E+04	1.54E+04
F8	Mean	-8.45E+02	-8.10E+02	7.42E+03	3.82E+02	-1.84E+02	-6.09E+02	1.71E+03	-7.44E+02	1.48E+02
	Std	1.84E+01	2.92E+01	9.27E+02	8.40E+01	1.70E+02	4.42E+01	4.56E+02	5.47E+01	3.17E+02
F9	Mean	-6.83E+02	-6.66E+02	3.13E+03	-6.02E+02	8.04E+02	-5.62E+02	-5.82E+02	-4.17E+02	-6.73E+02
	Std	1.83E+01	1.52E+01	3.64E+03	3.82E+01	1.21E+03	1.05E+02	3.09E+01	2.11E+02	1.55E+01
F10	Mean	-6.79E+02	-6.79E+02	-6.79E+02	-6.79E+02	-6.79E+02	-6.79E+02	-6.79E+02	-6.79E+02	-6.79E+02
	Std	3.75E-02	3.06E-02	3.68E-02	4.20E-02	3.24E-02	3.66E-02	3.07E-02	3.77E-02	4.25E-02
F11	Mean	-5.47E+02	-5.41E+02	-5.30E+02	-5.31E+02	-5.40E+02	-5.39E+02	-5.25E+02	-5.31E+02	-5.37E+02
	Std	4.72E+00	5.14E+00	1.94E+00	5.03E+00	3.49E+00	5.00E+00	2.10E+00	4.43E+00	5.80E+00
F12	Mean	-4.53E+02	-4.22E+02	1.07E+04	2.15E+03	1.11E+03	-4.25E+01	3.82E+03	-3.59E+02	1.49E+03
	Std	1.52E+01	5.95E+01	1.38E+03	1.11E+02	2.11E+02	1.03E+02	6.89E+02	4.04E+01	4.93E+02
F13	Mean	-3.12E+02	6.29E+01	6.40E+02	3.70E+02	2.44E+02	9.27E+01	3.54E+02	1.79E+02	1.66E+02
	Std	2.07E+01	4.35E+01	3.81E+01	7.29E+01	3.49E+01	6.36E+01	3.87E+01	8.96E+01	5.11E+01
F14	Mean	-1.01E+02	1.89E+02	8.09E+02	5.30E+02	6.08E+02	3.58E+02	4.96E+02	7.02E+02	2.74E+02
	Std	5.76E+01	6.99E+01	6.04E+01	6.84E+01	5.99E+01	7.95E+01	5.94E+01	8.71E+01	7.64E+01
F15	Mean	1.49E+02	4.17E+02	9.58E+02	7.21E+02	8.90E+02	6.19E+02	6.36E+02	8.65E+02	4.68E+02
	Std	5.03E+01	7.52E+01	5.91E+01	6.93E+01	7.56E+01	9.24E+01	6.28E+01	1.09E+02	8.22E+01
F16	Mean	2.82E+03	7.02E+03	1.42E+04	1.26E+04	7.97E+03	7.41E+03	1.38E+04	7.40E+03	1.04E+04
	Std	5.77E+02	7.27E+02	5.72E+02	1.20E+03	8.25E+02	1.14E+03	4.47E+02	1.27E+03	9.29E+02
F17	Mean	9.26E+03	9.42E+03	1.49E+04	1.30E+04	9.19E+03	1.04E+04	1.49E+04	1.11E+04	1.24E+04
	Std	9.92E+02	8.18E+02	4.64E+02	1.23E+03	4.95E+02	9.46E+02	3.93E+02	9.50E+02	1.15E+03
F18	Mean	2.03E+02	2.04E+02	2.04E+02	2.03E+02	2.00E+02	2.03E+02	2.04E+02	2.03E+02	2.04E+02
	Std	7.12E-01	5.23E-01	2.87E-01	5.11E-01	1.23E-02	7.26E-01	3.50E-01	4.13E-01	3.57E-01
F19	Mean	5.37E+02	8.49E+02	1.58E+03	1.27E+03	9.57E+02	1.15E+03	1.37E+03	1.54E+03	1.14E+03
	Std	3.87E+01	6.93E+01	5.22E+01	1.03E+02	7.87E+01	7.65E+01	8.15E+01	8.24E+01	7.82E+01
F20	Mean	7.68E+02	9.47E+02	1.71E+03	1.40E+03	1.03E+03	1.35E+03	1.46E+03	1.68E+03	1.31E+03
	Std	6.74E+01	5.04E+01	5.04E+01	1.15E+02	5.32E+01	9.80E+01	1.05E+02	5.44E+01	7.36E+01
F21	Mean	5.23E+02	5.37E+02	5.36E+05	1.61E+04	1.32E+04	6.12E+02	7.50E+04	5.86E+02	2.07E+04
	Std	5.30E+00	6.41E+00	1.32E+05	2.30E+03	3.32E+03	3.13E+01	4.11E+04	1.86E+01	4.51E+04
F22	Mean	6.22E+02	6.24E+02	6.25E+02	6.24E+02	6.25E+02	6.24E+02	6.24E+02	6.25E+02	6.24E+02
	Std	5.27E-01	8.25E-01	2.29E-01	5.91E-01	2.06E-01	5.65E-01	4.01E-01	1.98E-01	8.93E-01
F23	Mean	5.88E+02	6.15E+02	3.23E+04	6.60E+03	4.10E+03	8.57E+02	9.22E+03	6.92E+02	2.81E+03
	Std	4.31E+01	6.63E+01	3.32E+03	6.46E+02	4.63E+02	8.92E+01	1.73E+03	6.23E+01	8.85E+02
F24	Mean	6.31E+02	7.77E+02	1.14E+03	9.17E+02	8.38E+02	8.44E+02	1.09E+03	8.94E+02	8.88E+02
	Std	3.54E+01	3.21E+01	2.56E+01	4.24E+01	1.94E+01	3.66E+01	3.40E+01	2.75E+01	4.64E+01
F25	Mean	6.02E+02	6.57E+02	6.93E+02	6.78E+02	6.64E+02	6.62E+02	6.76E+02	6.72E+02	6.57E+02
	Std	7.33E-01	3.50E+00	5.33E+00	7.27E+00	3.37E+00	7.04E+00	6.58E+00	4.32E+00	9.23E+00
F26	Mean	9.11E+02	1.25E+03	1.89E+03	1.64E+03	1.39E+03	1.50E+03	1.72E+03	1.84E+03	1.47E+03
	Std	3.47E+01	8.70E+01	5.71E+01	1.37E+02	7.99E+01	1.10E+02	9.35E+01	8.66E+01	7.70E+01
F27	Mean	9.45E+02	1.09E+03	1.47E+03	1.26E+03	1.17E+03	1.16E+03	1.41E+03	1.18E+03	1.20E+03
	Std	4.72E+01	2.67E+01	2.75E+01	6.76E+01	1.86E+01	4.13E+01	3.54E+01	2.64E+01	5.17E+01
F28	Mean	2.05E+03	1.52E+04	3.52E+04	2.26E+04	1.17E+04	2.03E+04	2.67E+04	2.32E+04	1.79E+04
	Std	6.36E+02	3.68E+03	2.19E+03	3.44E+03	6.70E+02	4.20E+03	3.23E+03	2.83E+03	5.08E+03
F29	Mean	7.55E+03	8.00E+03	1.50E+04	1.21E+04	8.98E+03	8.76E+03	1.50E+04	9.03E+03	1.18E+04
	Std	7.43E+02	4.79E+02	3.83E+02	1.05E+03	9.58E+02	1.11E+03	3.25E+02	1.23E+03	9.83E+02

Table 8. Results of benchmark functions (F30-F57), with 50 dimensions

		SRO	PSO	BOA	BH	GSA	AO	SCA	HHO	STOA
F30	Mean	1.33E+03	1.44E+03	1.64E+04	5.37E+03	1.98E+04	1.89E+03	8.55E+03	1.52E+03	5.10E+03
	Std	8.16E+01	7.14E+01	2.48E+03	4.04E+02	1.88E+03	1.77E+02	1.25E+03	8.69E+01	1.66E+03
F31	Mean	5.43E+06	3.46E+07	4.30E+10	1.56E+10	5.47E+09	2.89E+08	1.62E+10	1.17E+08	4.44E+09
	Std	2.64E+06	4.17E+07	9.98E+09	2.11E+09	2.00E+09	1.50E+08	3.88E+09	7.43E+07	2.21E+09
F32	Mean	9.04E+03	1.38E+06	1.67E+10	4.23E+09	1.09E+08	3.83E+06	4.48E+09	3.02E+06	6.51E+08
	Std	1.02E+04	3.16E+06	7.77E+09	7.71E+08	2.51E+08	3.25E+06	1.71E+09	2.13E+06	6.11E+08
F33	Mean	1.31E+05	5.90E+05	1.17E+07	2.49E+06	6.38E+06	2.67E+06	3.81E+06	1.03E+06	9.82E+05
	Std	1.05E+05	2.28E+06	8.40E+06	5.49E+05	3.26E+06	2.07E+06	2.00E+06	6.51E+05	6.57E+05
F34	Mean	9.41E+03	2.38E+04	2.62E+09	2.69E+06	3.47E+07	3.95E+05	6.91E+08	4.66E+05	5.48E+07
	Std	6.03E+03	1.34E+04	1.39E+09	1.45E+06	6.88E+07	2.00E+05	2.68E+08	2.76E+05	1.12E+08
F35	Mean	3.31E+03	3.56E+03	8.50E+03	6.03E+03	4.77E+03	4.17E+03	5.84E+03	4.20E+03	3.98E+03
	Std	4.61E+02	4.30E+02	1.08E+03	5.63E+02	6.03E+02	5.87E+02	2.60E+02	4.78E+02	3.93E+02
F36	Mean	2.87E+03	3.32E+03	7.15E+03	3.59E+03	3.94E+03	3.52E+03	4.62E+03	3.71E+03	3.56E+03
	Std	3.52E+02	2.33E+02	2.01E+03	3.86E+02	3.28E+02	3.21E+02	3.21E+02	4.42E+02	3.32E+02
F37	Mean	2.12E+06	5.66E+05	3.22E+07	8.14E+06	8.98E+06	7.78E+06	2.80E+07	3.71E+06	6.16E+06
	Std	2.03E+06	2.48E+05	2.13E+07	1.08E+06	5.51E+06	5.02E+06	1.23E+07	2.96E+06	3.94E+06
F38	Mean	1.82E+04	6.17E+04	9.86E+08	7.90E+05	2.70E+05	1.79E+06	4.29E+08	8.80E+05	2.12E+07
	Std	1.10E+04	3.89E+04	6.36E+08	2.76E+05	1.17E+05	1.47E+06	1.97E+08	5.50E+05	4.29E+07
F39	Mean	3.00E+03	3.12E+03	4.13E+03	3.60E+03	3.60E+03	3.18E+03	4.10E+03	3.41E+03	3.37E+03
	Std	2.82E+02	2.42E+02	1.71E+02	2.95E+02	3.09E+02	3.24E+02	2.22E+02	2.58E+02	3.59E+02
F40	Mean	1.59E+03	1.59E+03	5.12E+03	3.91E+03	3.89E+03	2.04E+03	4.78E+03	1.64E+03	4.34E+03
	Std	3.56E+02	1.69E+02	6.01E+01	6.26E+01	8.33E+01	2.87E+02	1.55E+02	2.03E+02	3.04E+02
F41	Mean	3.95E+03	1.10E+04	1.65E+04	1.56E+04	1.40E+04	1.10E+04	1.56E+04	1.12E+04	1.24E+04
	Std	6.09E+02	1.47E+03	4.57E+02	6.99E+02	6.68E+02	7.86E+02	3.57E+02	1.26E+03	8.31E+02
F42	Mean	1.08E+04	1.26E+04	1.68E+04	1.61E+04	1.34E+04	1.30E+04	1.64E+04	1.41E+04	1.36E+04
	Std	1.20E+03	1.30E+03	2.93E+02	8.38E+02	5.00E+02	1.40E+03	3.70E+02	9.63E+02	1.28E+03
F43	Mean	1.34E+03	1.38E+03	1.55E+03	1.53E+03	2.02E+03	1.39E+03	1.43E+03	1.44E+03	1.37E+03
	Std	1.60E+01	1.78E+01	5.69E+01	2.33E+01	1.19E+02	1.21E+01	6.67E+00	3.01E+01	1.15E+01
F44	Mean	1.46E+03	1.56E+03	1.58E+03	1.65E+03	1.76E+03	1.53E+03	1.55E+030	1.56E+03	1.49E+03
	Std	1.27E+01	2.37E+01	2.01E+01	2.26E+01	2.54E+01	1.21E+01	7.17E+00	2.66E+01	1.06E+01
F45	Mean	1.44E+03	1.57E+03	1.46E+03	1.54E+03	1.68E+03	1.66E+03	1.64E+03	1.67E+03	1.65E+03
	Std	8.47E+01	1.20E+02	1.89E+01	1.35E+02	6.15E+01	4.81E+01	9.95E+01	5.18E+01	1.32E+01
F46	Mean	2.97E+03	3.34E+03	4.23E+03	3.90E+03	4.03E+03	3.41E+03	3.67E+03	3.65E+03	3.31E+03
	Std	1.15E+02	1.27E+02	1.90E+02	8.54E+01	1.30E+02	1.02E+02	5.11E+01	1.83E+02	1.47E+02
F47	Mean	2.46E+03	3.64E+03	9.68E+03	8.58E+03	9.98E+03	6.77E+03	7.12E+03	1.00E+04	5.63E+03
	Std	1.32E+03	2.06E+03	6.37E+02	5.28E+02	3.77E+02	1.27E+03	6.30E+02	8.44E+02	1.11E+03
F48	Mean	2.44E+03	2.68E+03	2.96E+03	2.96E+03	2.87E+03	2.70E+03	2.91E+03	2.85E+03	2.70E+03
	Std	2.55E+01	5.00E+01	1.15E+02	5.16E+01	3.13E+01	6.04E+01	4.27E+01	6.62E+01	4.45E+01
F49	Mean	9.06E+03	1.01E+04	1.49E+04	1.40E+04	1.23E+04	1.11E+04	1.65E+04	1.11E+04	1.36E+04
	Std	9.01E+02	9.74E+02	2.62E+03	1.20E+03	5.36E+02	1.11E+03	3.99E+02	9.39E+02	9.43E+02
F50	Mean	2.87E+03	3.52E+03	4.06E+03	4.12E+03	4.89E+03	3.37E+03	3.60E+03	3.70E+03	3.18E+03
	Std	3.11E+01	2.09E+02	1.24E+02	1.27E+02	1.68E+02	1.12E+02	6.51E+01	1.36E+02	6.99E+01
F51	Mean	3.04E+03	3.69E+03	5.06E+03	4.47E+03	4.58E+03	3.46E+03	3.77E+03	4.13E+03	3.27E+03
	Std	3.67E+01	1.34E+02	1.85E+02	1.34E+02	9.55E+01	1.00E+02	6.04E+01	1.78E+02	5.60E+01
F52	Mean	3.08E+03	3.11E+03	1.40E+04	5.55E+03	4.63E+03	3.30E+03	7.01E+03	3.18E+03	4.69E+03
	Std	2.65E+01	3.80E+01	6.32E+02	1.37E+02	2.31E+02	5.95E+01	7.94E+02	4.59E+01	5.09E+02
F53	Mean	5.39E+03	9.65E+03	1.62E+04	1.22E+04	1.23E+04	7.62E+03	1.26E+04	1.07E+04	8.15E+03
	Std	4.14E+02	2.97E+03	5.48E+02	9.12E+02	6.92E+02	2.78E+03	6.30E+02	1.89E+03	5.31E+02
F54	Mean	3.42E+03	3.90E+03	5.22E+03	5.97E+03	8.52E+03	3.98E+03	4.64E+03	4.30E+03	3.82E+03
	Std	8.14E+01	3.47E+02	4.28E+02	2.52E+02	7.50E+02	2.17E+02	1.85E+02	3.39E+02	1.36E+02
F55	Mean	3.36E+03	3.38E+03	1.20E+04	6.27E+03	5.93E+03	3.99E+03	7.45E+03	3.54E+03	8.80E+03
	Std	2.51E+01	1.40E+02	7.05E+02	1.35E+02	2.80E+02	3.10E+02	6.63E+02	6.51E+01	1.53E+03
F56	Mean	4.06E+03	5.85E+03	3.80E+04	8.94E+03	1.04E+04	6.44E+03	8.06E+03	5.76E+03	6.34E+03
	Std	2.55E+02	5.54E+02	2.43E+04	5.63E+02	3.35E+03	8.88E+02	8.22E+02	4.76E+02	7.42E+02
F57	Mean	1.04E+06	1.67E+07	2.35E+09	2.59E+08	2.28E+08	8.54E+07	8.34E+08	3.59E+07	2.77E+08
	Std	3.31E+05	8.17E+06	1.13E+09	1.51E+07	2.97E+07	3.15E+07	2.63E+08	7.55E+06	1.00E+08

4 Experiments on Real-world Engineering Problems

In this section, three real engineering design problems are handled using the SRO algorithm, and the results obtained are analyzed in comparison with other competing algorithms.

4.1 Tubular Column Design

As illustrated in Figure 3, the objective of the tube column design problem consists in designing a homogeneous tube column that can withstand stresses at a minimum cost. The optimization variables are the average diameter of the column $t(x_1)$ and the thickness of the tube $t(x_2)$. In addition, the object has a yield stress of $500kgf / cm^2$, a density of $0.0025kgf / cm^3$, and a modulus of elasticity of $0.85 \times 106kgf/cm^2$. The mathematical expressions are as follows.

$$f(x) = 9.8x_1x_2 + 2x_1. \quad \textbf{(24)}$$

The constraints are as follows:

$$g_1(X) = \frac{P}{\pi x_1 x_2 \sigma_y} - 1 \leq 0. \quad \textbf{(25)}$$

$$g_2(X) = \frac{8PL^2}{\pi^3 E x_1 x_2 (x_1^2 x_2^2)} - 1 \leq 0. \quad \textbf{(26)}$$

$$g_3(X) = \frac{2.0}{x_1} - 1 \leq 0. \quad \textbf{(27)}$$

$$g_4(X) = \frac{x_1}{14} - 1 \leq 0. \quad \textbf{(28)}$$

$$g_5(X) = \frac{2.0}{x_2} - 1 \leq 0. \quad \textbf{(29)}$$

$$g_6(X) = \frac{x_2}{8} - 1 \leq 0. \quad \textbf{(30)}$$

The range of variables is as follows:

$2 \leq x_1 \leq 14$

$0.2 \leq x_2 \leq 0.8$

The results of comparing the optimal solution obtained for this problem with other algorithms are shown in Table 9, and the statistics of this algorithm on this problem are shown in Table 10. It is concluded from the results in the table that SRO achieves good results on this problem for both the mean or mean squared difference values of the optimal solution.

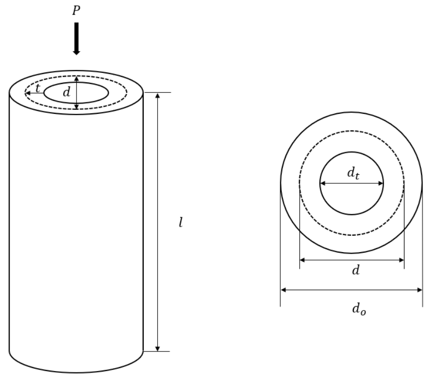

Figure 3. Tubular column design

Table 9. The best solution obtained from competitive algorithms for the tubular column design problem

Algorithms	x_1	x_2	f_cost
SRO	5.4522	0.2916	**26.4864**
GWO	5.4522	0.2916	26.488
PSO	5.4522	0.2916	26.48774
GSA	5.4407	0.2934	26.60487
BOA	5.4541	0.2915	26.53215
BH	5.454	0.2915	26.49516
AO	5.4531	0.2916	26.58591
SCA	5.4529	5.4529	26.5537
HHO	5.452	0.2917	26.5035
AOA	5.469	0.2937	27.7581

Table 10. The results obtained from competitive algorithms for the tubular column design problem

Algorithms	Mean	Std
SRO	**26.48636242**	**0.000000011**
GWO	26.48800186	0.000751542
PSO	26.4877424	0.001151451
GSA	26.60486993	0.056760976
BOA	26.53215283	0.022269774
BH	26.49515583	0.00269796
AO	26.58591384	0.057574278
SCA	26.55370079	0.048099527
HHO	26.50348647	0.014299812
AOA	27.75807917	0.429881546

4.2 Pressure Vessel Design

As Figure 4 shows that the goal of pressure vessel design is to meet production needs while minimizing the total cost $f(x)$. Their four design variables are shell thickness, head thickness, inner radius and container length. The objective function of the problem is as follows.

$$(l_1 = x_1,\ l_2 = x_2,\ l_3 = x_3,\ l_4 = x_4)$$

$$f(x) = 0.6224\, x_1 x_3 x_4 + 1.7781\, x_2 x_3^2 + 3.1661\, x_1^2 x_4 + 19.84 x_1^2 x_3 \quad \textbf{(31)}$$

Constraints:

$$g_1(x) = -x_1 + 0.0193x_3 \leq 0. \quad \textbf{(32)}$$

$$g_2(x) = -x_2 + 0.00945x_3 \leq 0. \quad \textbf{(33)}$$

$$g_3(x) = \pi x_3^2 x_4 - \frac{4}{3}\pi x_3^2 + 1296000 \le 0. \quad \textbf{(34)}$$

$$g_4(x) = x_4 - 240 \le 0. \quad \textbf{(35)}$$

The boundary constraints are as follows:
$0 \le x_1 \le 99$
$0 \le x_2 \le 99$
$10 \le x_3 \le 200$
$10 \le x_4 \le 200$

Similarly, the results of the optimal solution compared with other algorithms are shown in Table 11 and the statistical results are show in Table 12. From the results, it can still be concluded that SRO achieves good results for the mean or mean squared deviation values of the optimal solutions to this problem.

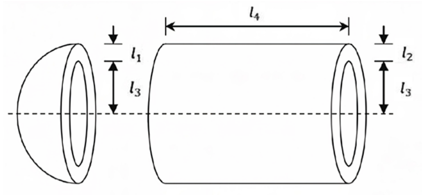

Figure 4. Pressure vessel design

Table 11. The best solution obtained from competitive algorithms for the pressure vessel design problem

Algorithms	x_1	x_2	x_3	x_4	f_cost
SRO	12.5325	6.8094	42.0984	176.6366	6059.71446
GWO	13.0352	6.7747	42.1007	176.6101	6319.830831
PSO	13.4187	6.8833	42.0983	176.6431	6281.177956
GSA	16.0081	7.7748	51.8186	84.541	6491.550472
BOA	13.9000	8.2522	45.1691	143.0469	6879.802502
BH	8.4580	8.4580	42.1115	176.4754	7186.614939
AO	12.8735	6.5319	42.0980	176.7507	6127.753493
HHO	13.0182	6.6231	42.099	176.6292	6532.194636
SCA	12.3536	5.824	40.3814	200	6545.596124
AOA	11.8463	6.0573	40.6493	200.0000	7378.927458

Table 12. The results obtained from competitive algorithms for the pressure vessel design problem

Algorithms	Mean	Std
SRO	**6062.60005**	**7.358546000**
GWO	6319.83083	536.499636
PSO	6281.178	212.4374
GSA	6491.55047	52.799929
BOA	6879.8025	290.137385
BH	7186.615	698.9884
AO	6127.753	133.1123
SCA	6545.596	497.6136
HHO	6532.19464	373.518119
AOA	7378.92746	967.85382

4.3 Welded Beam Design Problem

As Figure 5 shows that the welded beam design works with four variables. The thickness of weld ($l_1 = x_1$), the length of the clamped bar ($l_2 = x_2$), height of the bar ($l_3 = x_3$), and thickness of the bar ($l_4 = x_4$). To minimize the total manufacturing cost (f_1) and the deflection of the beam (f_2) are the objectives under the appropriate constraints and search space.

$$f_1(x) = 1.10471 x_1^2 x_2 + 0.04811 x_3 x_4 (14 + x_2). \quad \textbf{(36)}$$

$$f_2(x) = 2.1925 / x_3^3 x_4. \quad \textbf{(37)}$$

The constraints are as follows:

$$g_1(x) = tau(x) - 13600 \le 0. \quad \textbf{(38)}$$

$$g_2(x) = sig(x) - 30000 \le 0. \quad \textbf{(39)}$$

$$g_3(x) = x_1 - x_4 \le 0. \quad \textbf{(40)}$$

$$g_4(x) = 6000 - P_c(x) \le 0. \quad \textbf{(41)}$$

$$P_c(x) = \left(\frac{4.013E\sqrt{\frac{x_3^2 x_4^6}{36}}}{L^2}\right)\left(1 - \left(\left(\frac{x_3}{2L}\right)\sqrt{\frac{E}{4G}}\right)\right). \quad \textbf{(42)}$$

$$del = \frac{4PL^3}{E x_3^2 x_4}. \quad \textbf{(43)}$$

$$sig(x) = \frac{6PL}{x_4 x_3^2}. \quad \textbf{(44)}$$

$$R = \sqrt{(\frac{x_2^2}{4}) + (\frac{x_1 + x_3}{2})^2}. \quad \textbf{(45)}$$

$$M1 = P * (L + \frac{x_2}{2}). \quad \textbf{(46)}$$

$$tau2(x) = \frac{M1R}{J}. \quad \textbf{(47)}$$

$$tau1(x) = \frac{P}{\sqrt{2}x_1 x_2}. \quad \textbf{(48)}$$

$$tau(x) = \sqrt{\begin{array}{l} tau1^2(x) + 2 \cdot tau1(x) \cdot tau2(x) \cdot \dfrac{x_2}{2R} \\ + tau2^2(x) \end{array}}. \quad \textbf{(49)}$$

The average result of the optimal solution compared to other algorithms is 1.72487, which is the optimal algorithm in comparison with the other eight algorithms, as shown in Table 13. The statistical results are shown in Table 14. From the results, the algorithm's ability to get the optimal value shows good performance in terms of both optimal value and stability.

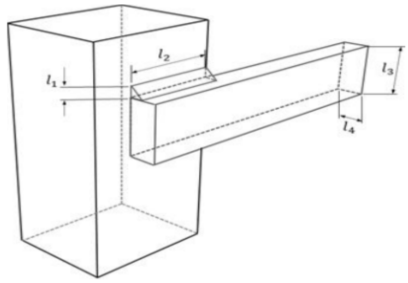

Figure 5. Welded beam design problem

Table 13. The best solution obtained from competitive algorithms for the welded beam design

Algorithms	x_1	x_2	x_3	x_4	x_5
SRO	0.2057	3.4705	9.0366	0.2057	**1.72487**
GWO	0.2058	3.4697	9.0379	0.2057	1.72606
PSO	0.2058	3.4686	9.0396	0.2058	1.879417
GSA	0.2143	3.8903	8.7201	0.2279	2.100498
BOA	0.2295	3.2134	8.5366	0.2445	2.377411
BH	0.234	3.2779	8.4697	0.2342	2.0929599
AO	0.2046	3.5737	8.9134	0.2123	1.928483
SCA	0.2128	3.4794	8.8981	0.2128	1.8202804
HHO	0.2062	3.4372	9.0999	0.2061	1.82235
AOA	0.2055	3.4838	9.0336	0.206	2.39703

Table 14. The results obtained from competitive algorithms for the welded beam design problem

Algorithms	Mean	Std
SRO	**1.72489491**	**0.000032701**
GWO	1.72606	0.000696
PSO	1.879417	0.228365
GSA	2.100498	0.125531
BOA	2.377411	0.300632
BH	2.09296	0.127019
AO	1.928483	0.144891
SCA	1.82028	0.031162
HHO	1.82235	0.089309
AOA	2.39703	0.178782

5 Conclusions

In this study, a new algorithm based on the ship rescue phenomenon, known as SRO, is proposed. To evaluate the performance of SRO, a new test suite consisting of the CEC2013 test suite and the CEC2017 test suite and three engineering optimization problems are extensively investigated. In most cases, SRO obtains results that highly outperform other known and state-of-the-art metaheuristics and can avoid falling into local optima. Future research should modify SRO in different ways, such as binary and multi-objectives strategies. In addition, it is useful to apply SRO to practical optimization problems, such as image processing and so on.

References

[1] T. Yamamoto, Historical developments in convergence analysis for newton's and newton-like methods, *Journal of Computational and Applied Mathematics*, Vol. 124, No. 1-2, pp. 1-23, December, 2000.

[2] S. M. Goldfeld, R. E. Quandt, H. F. Trotter, Maximization by quadratic hill-climbing, *Econometrica: Journal of the Econometric Society*, Vol. 34, No. 3, pp. 541-551, July, 1966.

[3] J. H. Holland, Genetic algorithms, Scientific American, Vol. 267, No. 1, pp. 66-73, July, 1992.

[4] M. Dorigo, M. Birattari, T. Stutzle, Ant colony optimization, *IEEE computational intelligence*

magazine, Vol. 1, No. 4, pp. 28-39, November, 2006.
[5] X.-S. Yang, A. H. Gandomi, Bat algorithm: a novel approach for global engineering optimization, *Engineering Computations*, Vol. 29, No. 5, pp. 464-483, July, 2012.
[6] Eberhart, Y. Shi, Particle swarm optimization: developments, applications and resources, *Proceedings of the 2001 congress on evolutionary computation (IEEE Cat. No. 01TH8546)*, Seoul, Korea (South), 2001, pp. 81-86.
[7] L. Abualigah, D. Yousri, M. Abd Elaziz, A. A. Ewees, M. A. Al-Qaness, A. H. Gandomi, Aquila optimizer: a novel meta-heuristic optimization algorithm, *Computers & Industrial Engineering*, Vol. 157, Article No. 107250, July, 2021.
[8] A. K. Qin, V. L. Huang, P. N. Suganthan, Differential evolution algorithm with strategy adaptation for global numerical optimization, *IEEE transactions on Evolutionary Computation*, Vol. 13, No. 2, pp. 398-417, April, 2009.
[9] Z. Meng, J.-S. Pan, K.-K. Tseng, Pade: An enhanced differential evolution algorithm with novel control parameter adaptation schemes for numerical optimization, *Knowledge-Based Systems*, Vol. 168, pp. 80-99, March, 2019.
[10] D. Karaboga, Artificial bee colony algorithm, *scholarpedia*, Vol. 5, No. 3, Article No. 6915, 2010.
[11] A. H. Alaidi, C. S. Der, Y. W. Leong, Systematic review of enhancement of artificial bee colony algorithm using ant colony pheromone, *International Journal of Interactive Mobile Technologies*, Vol. 15, No. 16, pp. 172-180, 2021.
[12] S. Mirjalili, S. M. Mirjalili, A. Lewis, Grey wolf optimizer, *Advances in engineering software*, Vol. 69, pp. 46-61, March, 2014.
[13] M. H. Nadimi-Shahraki, S. Taghian, S. Mirjalili, An improved grey wolf optimizer for solving engineering problems, *Expert Systems with Applications*, Vol. 166, Article No. 113917, March, 2021.
[14] T.-T. Nguyen, J.-S. Pan, T.-K Dao, A Compact Bat Algorithm for Unequal Clustering in Wireless Sensor Networks, *Applied Sciences*, Vol. 9, No. 10, Article No. 1973, May, 2019.
[15] J. Li, M. Gao, J.-S. Pan, S.-C. Chu, A parallel compact cat swarm optimization and its application in DV-Hop node localization for wireless sensor network, *Wireless Networks*, Vol. 27, No. 3, pp. 2081-2101, April, 2021.
[16] A. A. Heidari, S. Mirjalili, H. Faris, I. Aljarah, M. Mafarja, H. Chen, Harris hawks optimization: Algorithm and applications, *Future generation computer systems*, Vol, 97, pp. 849-872, August, 2019.
[17] G. Dhiman, A. Kaur, Stoa: a bio-inspired based optimization algorithm for industrial engineering problems, *Engineering Applications of Artificial Intelligence*, Vol. 82, pp. 148-174, June, 2019.
[18] A. Kaveh, N. Farhoudi, A new optimization method: Dolphin echolocation, *Advances in Engineering Software*, Vol. 59, pp. 53-70, May, 2013.
[19] Z. W. Geem, J. H. Kim, G. V. Loganathan, A new heuristic optimization algorithm: harmony search, *Simulation*, Vol. 76, No. 2, pp. 60-68, February, 2001.
[20] P. J. M. Van Laarhoven, E. H. L. Aarts, Simulated annealing, in: *Simulated annealing: Theory and applications, Mathematics and Its Applications*, Vol. 37, Springer, Dordrecht, 1987, pp. 7-15.
[21] E. Rashedi, H. Nezamabadi-Pour, S. Saryazdi, Gsa: a gravitational search algorithm, *Information sciences*, Vol. 179, No. 13, pp. 2232-2248, June, 2009.
[22] O. Bozorg-Haddad, M. Janbaz, H. A. Lóaiciga, Application of the gravity search algorithm to multi-reservoir operation optimization, *Advances in water resources*, Vol. 98, pp. 173-185, December, 2016.
[23] F. A. Hashim, E. H. Houssein, M. Mabrouk, W. Al-Atabany, S. Mirjalili, Henry gas solubility optimization: A novel physics-based algorithm, *Future Generation Computer Systems*, Vol. 101, pp. 646-667, December, 2019.
[24] F. A. Hashim, K. Hussain, E. H. Houssein, M. S. Mabrouk, W. Al-Atabany, Archimedes optimization algorithm: a new metaheuristic algorithm for solving optimization problems, *Applied Intelligence*, Vol. 51, No. 3, pp. 1531-1551, March, 2021.
[25] M. H. Mozaffari, H. Abdy, S. H. Zahiri, Ipo: an inclined planes system optimization algorithm, *Computing and Informatics*, Vol, 35, No, 1, pp. 222-240, 2016.
[26] A. Hatamlou, Black hole: A new heuristic optimization approach for data clustering, *Information sciences*, Vol. 222, pp. 175-184, February, 2013.
[27] V. Muthiah-Nakarajan, M. M. Noel, Galactic swarm optimization: a new global optimization metaheuristic inspired by galactic motion, *Applied Soft Computing*, Vol. 38, pp. 771-787, January, 2016.
[28] S. Mirjalili, S. M. Mirjalili, A. Hatamlou, Multi-verse optimizer: a nature-inspired algorithm for global optimization, *Neural Computing and Applications*, Vol. 27, No. 2, pp. 495-513, February, 2016.
[29] M. D. Li, H. Zhao, X. W. Weng, T. Han, A novel nature-inspired algorithm for optimization: Virus colony search, *Advances in engineering software*, Vol. 92, pp. 65-88, February, 2016.
[30] P. Civicioglu, Backtracking search optimization algorithm for numerical optimization problems, *Applied Mathematics and computation*, Vol. 219, No. 15, pp. 8121-8144, April, 2013.
[31] H. R. R. Zaman, F. S. Gharehchopogh, An improved particle swarm optimization with backtracking search optimization algorithm for solving continuous optimization problems, *Engineering with Computers*, Vol. 38, No. 4, pp. 2797-2831, October, 2022.
[32] H. Eskandar, A. Sadollah, A. Bahreininejad, M. Hamdi, Water cycle algorithm–a novel metaheuristic optimization method for solving constrained engineering optimization problems, Computers & Structures, Vol. 110-111, pp. 151-166, November, 2012.
[33] R. V. Rao, V. J. Savsani, D. Vakharia, Teaching–learning-based optimization: a novel method for constrained mechanical design optimization problems, *Computer-aided design*, Vol. 43, No. 3, pp. 303-315, March, 2011.
[34] H. Shah-Hosseini, The intelligent water drops algorithm:

a nature-inspired swarm-based optimization algorithm, *International Journal of Bio-inspired computation*, Vol. 1, No. 1-2, pp. 71-79, January, 2009.

[35] J. Zhang, M. Xiao, L. Gao, Q. Pan, Queuing search algorithm: A novel metaheuristic algorithm for solving engineering optimization problems, *Applied Mathematical Modelling*, Vol. 63, pp. 464-490, November, 2018.

[36] N. Gunantara, A review of multi-objective optimization: Methods and its applications, *Cogent Engineering*, Vol. 5, No. 1, Article No. 1502242, 2018

[37] K. Guo, L. Zhang, Multi-objective optimization for improved project management: Current status and future directions, *Automation in Construction*, Vol. 139, Article No. 104256, July, 2022.

[38] X.-F. Ji, J.-S. Pan, S.-C. Chu, P. Hu, Q.-W. Chai, P. Zhang, Adaptive cat swarm optimization algorithm and its applications in vehicle routing problems, *Mathematical Problems in Engineering*, Vol. 2020, Article No. 1291526, April, 2020.

[39] X. Xue, J. Zhang, Matching large-scale biomedical ontologies with central concept based partitioning algorithm and adaptive compact evolutionary algorithm, *Applied Soft Computing*, Vol. 106, pp. 107343, July, 2021.

[40] S. Mirjalili, Sca: a sine cosine algorithm for solving optimization problems, *Knowledge-based systems*, Vol. 96, pp. 120-133, March, 2016.

[41] S. Arora, S. Singh, Butterfly optimization algorithm: a novel approach for global optimization, *Soft Computing*, Vol. 23, No. 3, pp. 715-734, February, 2019.

[42] J.-S. Pan, P. Hu, S.-C. Chu, Binary fish migration optimization for solving unit commitment, *Energy*, Vol. 226, Article No. 120329, July, 2021.

[43] J.-S. Pan, J. Wang, J. Lai, H. Luo, S.-C. Chu, A Modes Communication of Cat Swarm Optimization Based WSN Node Location Algorithm, *Journal of Internet Technology*, Vol. 22, No. 5, pp. 949-956, September, 2021.

[44] P. Hu, J.-S. Pan, S.-C. Chu, C. Sun, Multi-surrogate assisted binary particle swarm optimization algorithm and its application for feature selection, *Applied Soft Computing*, Vol. 121, Article No. 108736, May, 2022.

[45] C. Wu, S. Fu, T. Li, Research of the wsn routing based on artificial bee colony algorithm, *Journal of Information Hiding and Multimedia Signal Processing*, Vol. 8, No. 1, pp. 120-126, January, 2017.

[46] P.-C. Song, S.-C. Chu, J.-S. Pan, H. Yang, Simplified Phasmatodea population evolution algorithm for optimization, *Complex & Intelligent Systems*, Vol. 8, No. 4, pp. 2749-2767, August, 2022.

Biographies

Shu-Chuan Chu received the Ph.D. degree from the School of Computer Science, Engineering and Mathematics, Flinders University, Australia, in 2004. She joined Flinders University, in December 2009, after nine years at Cheng Shiu University, Taiwan. She has been a Research Fellow with the College of Science and Engineering, Flinders University, since December 2009. She has been a Research Fellow, with PhD advisor, at the College of Computer Science and Engineering, Shandong University of Science and Technology, since September 2019. Her research interests mainly include swarm intelligence, watermarking, and wireless sensor networks.

Ting-Ting Wang received her B.S. degree from Shandong Women's University, China. She is currently pursuing the master degree with the Shandong University of Science and Technology, Qingdao, China. Her recent research interests include swarm intelligence, and image processing.

Ali Riza Yildiz is currently a Professor with the Department of Automotive Engineering, Bursa Uludağ University, Bursa, Turkey. He is a member of the Turkish Academy of Sciences (TUBA). His research interests include shape and topology optimization of vehicle components, meta-heuristic optimization techniques, and reliability-based design optimization. He has been serving as an associate editor for the SCI journals.

Jeng-Shyang Pan received the B.S. degree in electronic engineering from the National Taiwan University of Science and Technology in 1986, the M.S. degree in communication engineering from National Chiao Tung University, Taiwan, in 1988, and the Ph.D. degree in electrical engineering from the University of Edinburgh, U.K., in 1996. He is currently the Professor of Shandong University of Science and Technology. He is the IET Fellow, U.K., and has been the Vice Chair of the IEEE Tainan Section and Tainan Chapter Chair of IEEE Signal Processing Society. His current research interest includes the information hiding, artificial intelligence and wireless sensor networks.